inorganics

MDPI

Review

Mechanochemical Synthesis of Solid-State Electrolytes

Sanja Burazer * and Jasminka Popović *

Ruđer Bošković Institute, Bijenička Cesta 54, 10000 Zagreb, Croatia
* Correspondence: sanja.burazer@irb.hr (S.B.); jasminka.popovic@irb.hr (J.P.)

Abstract: In recent decades, the field of materials research has put significant emphasis on developing innovative platforms that have the potential to address the increasing global energy demand. Batteries have demonstrated their enormous effectiveness in the context of energy storage and consumption. However, safety issues associated with liquid electrolytes combined with a low abundance of lithium in the Earth's crust gave rise to the development of solid-state electrolytes and cations other than lithium. The commercial production of solid-state batteries demands the scaling up of solid-state electrolyte syntheses as well as the mixing of electrode composites containing solid electrolytes. This review is motivated by the recent literature, and it gives a thorough overview of solid-state electrolytes and highlights the significance of the employed milling and dispersing procedures for the resulting ionic transport properties.

Keywords: solid-state electrolytes; all-solid-state batteries; mechanochemical synthesis; electrode/solid electrolyte interface; ionic conductivity

1. Introduction

Global warming, unsustainable usage of fossil fuels, and the everyday increase in the energetic needs of today's modern society, together with the world energy crisis, are in great need of a transition towards a sustainable energy system. Batteries proved to be of paramount importance for energy storage and consumption issues [1,2]. This is confirmed by the fact that the European Union (EU) aims to heavily boost the production of batteries by building 25–30 battery gigafactories across Europe with a capacity of approximately 400 gigawatt-hours (GWh) by 2025. It is expected that battery demand from EVs produced in Europe will reach 1200 GWh per year by 2040. In comparison with the previous period, that is more than five times the capacity of the gigafactory projects operating or under development on the continent last year [3].

Indeed, lithium-ion batteries (LiBs) boosted the development of mobile electronic equipment and electrical vehicles (EVs) with characteristics such as high energy density, low self-discharge (about 5% per month, while supercapacitors have a self-discharge of around 50% per month) [4], fast charge cycle (around 50% recharged in less than 25 min) [5], and long lifespan (most power tool manufacturers claim you should expect to obtain over 1000 charge cycles out of any given battery) [6]. LiBs are efficient, lightweight, and rechargeable power sources, applicable in portable electronic gadgets, medical devices, cars, and the aerospace industry, as well as for large-scale energy storage facilities [2]. The turning point certainly was the development of rechargeable pouch-type lithium batteries with a record-breaking energy density of over 700 Wh kg^{-1}, which is an enormous development in comparison with average lithium-ion batteries (260–270 wh/kg) or lead–acid batteries (50–100 wh/kg). This new design includes a high-capacity lithium-rich manganese-based cathode and a thin lithium metal anode with high specific energy [7]. Lithium nickel manganese cobalt oxides (NMCs) have been identified as promising candidates for achieving high energy density in future LIBs for EVs. These NMCs have the potential to reach an energy density of approximately 900 Wh kg^{-1}. Conversion-type alternative cathode materials, such as FeF_2 and FeF_3, have not been successfully developed due to significant

Citation: Burazer, S.; Popović, J. Mechanochemical Synthesis of Solid-State Electrolytes. *Inorganics* **2024**, *12*, 54. https://doi.org/10.3390/inorganics12020054

Academic Editor: Faxing Wang

Received: 20 December 2023
Revised: 1 February 2024
Accepted: 3 February 2024
Published: 6 February 2024

capacity degradation, despite their promise of achieving an ultrahigh energy density of up to 1500 Wh kg^{-1}. Si-based anode materials have shown promise as anode materials due to their high specific capacity of 4200 mAh g [8,9].

Over the years, many different electrode chemical compositions and structures have been explored to enhance and optimize the overall battery performance. Research by Kim and co-authors reports a $Li[Ni_{0.92}Co_{0.06}Al_{0.01}Nb_{0.01}]O_2$ (Nb-NCA93) cathode with a high energy density of 869 Wh kg^{-1}, where the presence of Nb induces the grain refinement of its secondary particles. This reduces internal stress and prevents variations in lithium concentration while cycling. A full cell obtained from the process achieves complete charging in about 12 min and maintains 85.3% of its original capacity even after undergoing 1000 cycles with complete discharge [10]. An example where initial capacity is retained at high values is the paper of Bijelić and co-authors, where as-prepared $ZnMn_2O_4$ showed a specific capacity of 909 mA h g^{-1} after 500 cycles, while the heat-treated spinel at 300 °C retained 1179 mA h g^{-1} (101% of its initial capacity). Also, it has been demonstrated that electrochemical performances can be significantly improved by controlling microstructural parameters [11]. For example, $CoMn_2O_4$ particle sizes are easily fine-tuned by applying different annealing temperatures; the particle size increases with increasing annealing temperature. However, contrary to the common assumption that nanostructuring the anode material improves battery performance, samples with the largest particle sizes can exhibit enhanced performance with a capacity retention of 104% after 1000 cycles (compared to the 2nd cycle) [12]. Despite the many breakthroughs that have been achieved, there are still many problems that prevent LiBs from successfully answering today's energy demands. First, there is an issue of high cost accompanied by the low abundance of metallic lithium in the Earth's crust, as well as the common utilization of highly flammable organic liquid electrolytes or polymer electrolytes. LiBs are generally characterized by inadequate thermal stability, which can cause gas production and leakage of the liquid electrolytes when operating at high voltages and/or elevated temperatures [13]. Therefore, it became obvious that the development of other energy storage technologies belonging to the post-lithium generation, such as Na, Mg, or Ca batteries, is much needed. Additionally, Zn-based batteries are making ongoing progress. In the research of Li and co-authors, a high-performance zinc–organic battery was achieved by tuning the electron delocalization within a designed fully conjugated two-dimensional hydrogen-bonded organic framework as a cathode material, resulting in a reversible capacity of 498.6 mAh g^{-1} at 0.2 A g^{-1}, good cyclability, and high energy density (355 Wh kg^{-1}) [14]. Additionally, through the research of Wei and co-authors, it has been demonstrated that iodine-loaded mesoporous poly(3,4-ethylenedioxythiophene):poly(styrenesulfonate) PEDOT:PSS nanospheres can serve as a promising cathode for aqueous zinc–iodine batteries with high specific capacity (241 mAh g^{-1}), excellent rate performance, and a superlong 20,000-cycle life [15]. All of the above-mentioned metals are considered cheaper and more abundant, and, additionally, with bivalent ions, it is possible to achieve a potentially higher energy density [16].

For both Li and other battery technologies, the inadequate safety of liquid electrolytes still poses a great issue that must be resolved. A potential solution can be found in the development of all-solid-state batteries (ASSBs), in which currently used liquid electrolytes would be replaced with solid-state electrolytes, resolving the problems of electrolyte decomposition and dendrite formation, a potential cause of short-circuits and fire, with additional improvement in energy density [17,18]. Additionally, it is expected that ASSBs will enable an increase in energy storage capacity by using metallic negative electrodes and positive electrodes operating at significantly higher potentials. Also, by removing the separator and current collector from the negative electrode, the battery design becomes more compact, making battery production simpler and cheaper [19,20]. The ideal solid electrolyte (SE) should possess high ionic conductivity, while electronic conductivity should be low, so that only metallic ions of interest are mobile between electrodes [21]. The challenging task is to design a solid electrolyte capable of conducting ions at room temperature (RT), exhibiting a sufficiently high ionic conductivity above 10^{-3} S cm^{-1} at RT and low activation

energy [22,23]. Some of the reported superionic conductors with conductivities of 10^{-6} to a record 10^{-2} S cm^{-1}, which is close to or even higher than that of liquid electrolytes, include polymer electrolytes [24–33], oxide electrolytes [34–44], sulfide electrolytes [44–57], hydrides [20,22,58–67], glass-ceramics [68], and recently revived halide electrolytes (Li_3MX_6, where M = Y and In; and X = Cl, Br, and I) [69–72].

The additional aspect worth exploring and aiming for a sustainable, cleaner environment is certainly related to the development of alternatives to traditional liquid-phase-based reactions [42,73–76], such as solvent-free and environmentally friendly mechanochemical synthesis. Mechanochemistry promotes physical and chemical transformations through the utilization of mechanical energy to design complex molecules and nanostructured materials. Additionally, it encourages dispersion and recombination of multiphase components and accelerates reaction rates and efficiencies via highly reactive surfaces [77,78]. Mechanochemical synthesis has various applications, including the preparation, functionalization, and transformation of metal–organic frameworks [79–88], different metal hydrides [89–113], (bi)metallic imidazolate compounds [114–116], and other energy storage materials, which are synthesized mechanochemically. Lately, mixing/milling techniques have been widely used in the mechanochemical synthesis of solid electrolytes and the processing of cathode composites, e.g., the preparation of functional composite materials and the production of ASSB components, even at a large scale [16,24,29,36,78,85,117–126]. Recent studies have demonstrated that mechanical milling has the potential to significantly enhance conductivity by five orders of magnitude at ambient temperature; this remarkable improvement renders mechanical milling an attractive technique for utilization in ASSBs [127]. It is also well known that composite formation can have a great impact on electrode performance [128–134].

As reported in our earlier paper, the presence of a Nafion® layer at a gold electrode considerably diminishes nucleation overpotential, resulting in a higher efficiency of the complete electrode reaction, which is applicable in the construction of high-efficiency and high-power positive electrodes in lead–acid batteries and supercapacitors [135]. Also, multilayer niobium diselenide (NbSe2)@graphene composite material was synthesized by ball milling and reported by Nguyen et al. as a new type of anode material for half-cell and full-cell LIBs, showing excellent electrochemical performance [136].

This paper aims to discuss the problems related to the manufacturing and implementation of solid-state electrolytes and to provide views on some of the most relevant questions under active discussion, such as exploring which type of solid electrolytes can be prepared by environmentally friendly mechanochemical synthesis; examining how mechanochemistry can help in overcoming chemical and mechanical stability issues in solid-state batteries; and, finally, assessing which solid-state electrolyte comes closest to fulfilling the expectations of safe energy storage systems.

2. Results and Discussion

2.1. Difference between Batteries with Liquid and Solid Electrolytes

Conventional liquid batteries have electrodes bathed in a liquid electrolyte, which allows positive ions (lithium, sodium, magnesium) to move from one electrode to another. When a liquid electrolyte is replaced by a solid one, the battery becomes all-solid-state. However, this brings some issues regarding the contact between the electrodes and the electrolyte, which is that in the case of liquid electrolytes, the contact is naturally good, but with two solid materials, the contact is often rather non-optimal. The interaction between the electrodes and the electrolyte must be strong; thus, in the case of a solid electrolyte, some pressure is often applied to maintain good contact between the components of the battery. These batteries are more compact and can be manufactured in smaller dimensions, often decreasing manufacturing costs [137].

It is expected that solid-state electrolytes possess four distinct characteristics for the desired electrochemical performance to be achieved. These include high ionic conductivity; low-cost raw materials and simple processing methods; adequate structural integrity,

mechanical strength, and few enough structural defects to prevent dendrite penetration; and low activation energy for ionic diffusion. Research is currently focused on overcoming three key difficulties, i.e., finding high-ionic-conductivity electrolytes, producing efficient electrodes, and improving the electrode–electrolyte interface to fulfill all of these particular needs of SSEs (Figure 1) [138,139].

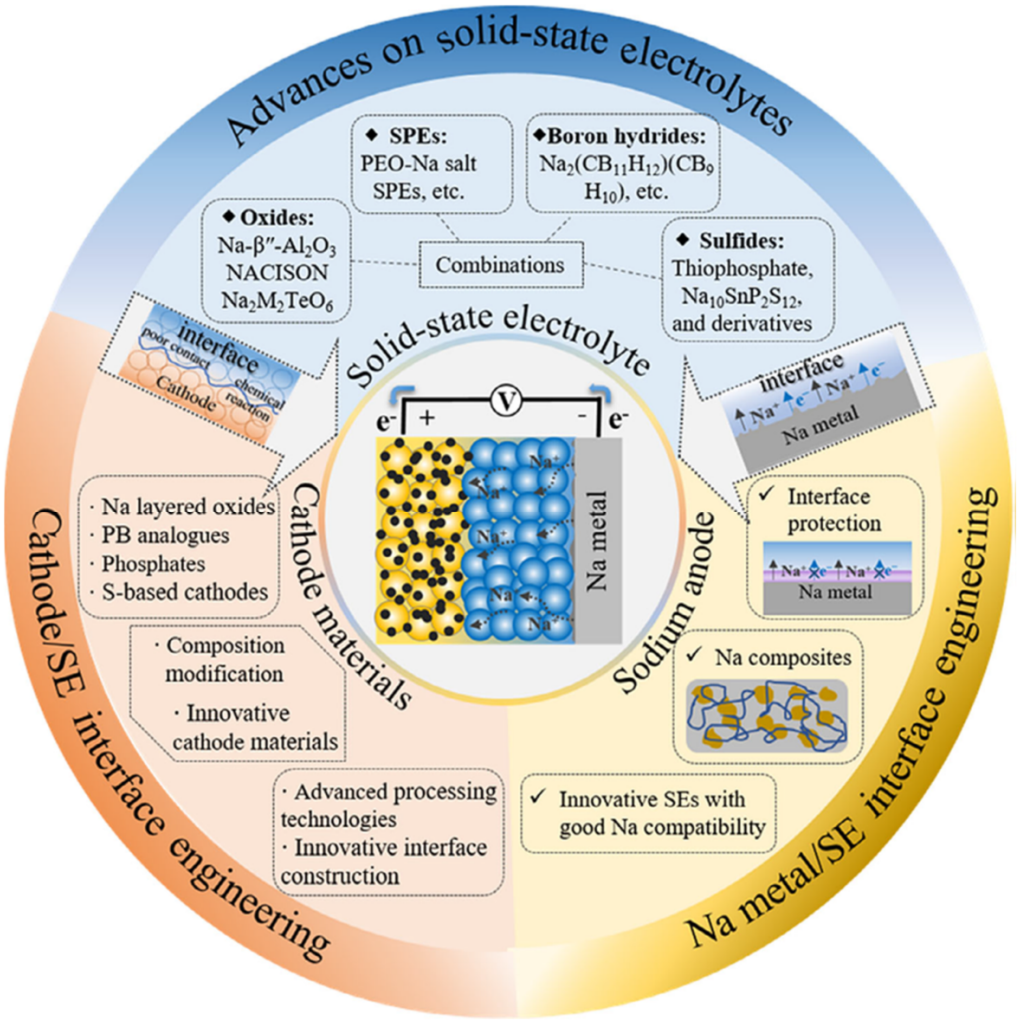

Figure 1. Schematic diagram of study trends for ASSBs. Reprinted with permission from [139]. https://doi.org/10.1002/aesr.202000057. https://creativecommons.org/licenses/by/4.0/ (accessed on 20 December 2023).

2.2. Types of Solid-State Electrolytes

Solid-state electrolytes can be grouped into solid inorganic electrolytes (SIEs), solid polymer electrolytes (organic electrolytes) (SPEs), and composite solid electrolytes (CSEs) (Figure 2) [128].

The first group is composed only of inorganic materials like ceramics and glass; the second contains a high-molecular-weight polymer matrix and a dissolved metal salt; and the last contains a solid polymer and inorganics [25,138–141].

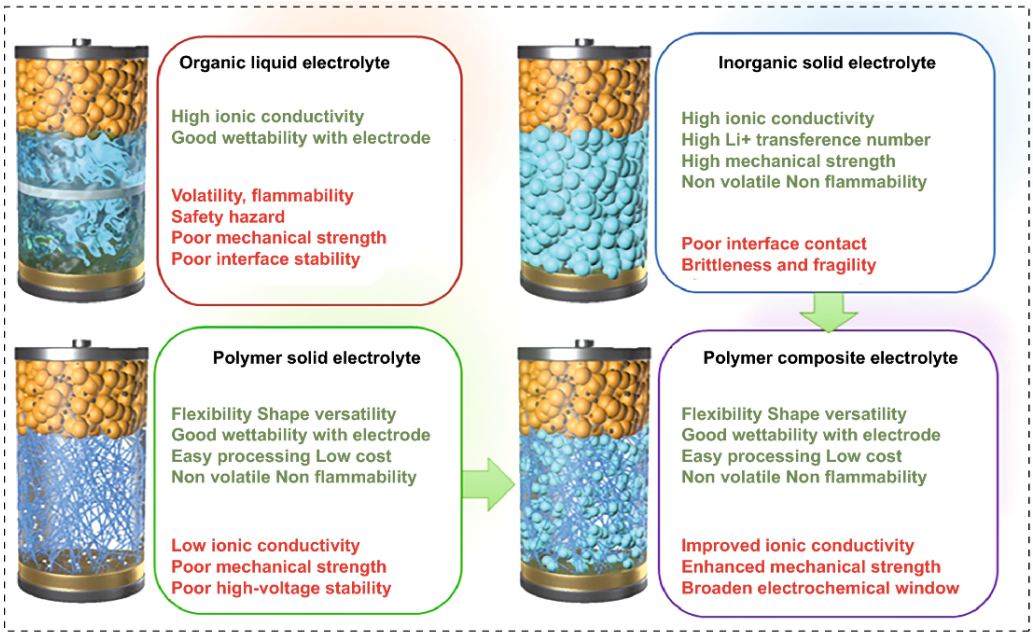

Figure 2. Performance comparison of different electrolytes. Reprinted with permission from [128]. https://doi.org/10.1007/s40820-022-00996-1. https://creativecommons.org/licenses/by/4.0/ (accessed on 20 December 2023).

Inorganic electrolytes typically demonstrate a notable ion conductivity above 10^{-4} S cm^{-1}, accompanied by remarkable thermal stability due to their rigid crystal structures [142]. Sometimes, the ionic conductivity of inorganic electrolytes is comparable with, or even higher than, that of liquid electrolytes [143]. The drawback of ASSBs with inorganic electrolytes is their low performance due to the poor interfacial contact between electrode and electrolyte [144,145]. Although organic electrolytes can be used for flexible battery design because of their soft intrinsic characteristics, they show lower conductivity as well as oxidation at high voltages and large ionic transfer resistance [146,147]. According to certain studies, the utilization of ceramic/polymer composite electrolytes has the potential to effectively address the challenges associated with ionic conductivity and interfacial contact. This is achieved by leveraging the respective benefits offered by these two distinct forms of electrolytes [138].

2.2.1. Solid Inorganic Electrolytes

When talking about inorganic solid electrolytes, the most popular types are LISICON (lithium super ionic conductor), LiPON (lithium phosphorus oxynitride), Li_3N, sulfide, argyrodite, garnet, perovskite, anti-perovskite, and NASICON (sodium super ionic conductor) (Figure 3b) [148–152]. The first LISICON-type solid electrolyte, $Li_{14}Zn(GeO_4)_4$, showed an ionic conductivity of 1.25×10^{-1} S cm^{-1} at 300 °C, as reported by Hong et al. [153]. LiPON is typically an amorphous Li-ion solid electrolyte with an ionic conductivity of about 2×10^{-6} S cm^{-1} at 25 °C, and it is stable with lithium [154].

Several metal cations can be found in SIE, with lithium certainly being the most popular one; however, considering the drawbacks of lithium usage mentioned in the introduction, post-lithium solutions have to be sought. As the logical post-lithium solution for electrochemical energy storage, sodium is the first on the list; it is very abundant, inexpensive, and evenly distributed on Earth [17,155–160]. Every day, an increase in battery demand causes an increase in the price of lithium. The data provided by S&P Global Commodity Insights indicate a substantial increase of almost 450% compared to the corresponding period of the previous year. On the other hand, sodium has an almost unlimited supply (almost 500 times more than lithium in the Earth's crust, and it can be extracted from seawater); therefore, it might provide a less expensive and more environmentally

friendly alternative. Another advantage of post-lithium technologies is their safety because sodium batteries are non-flammable and less sensitive to temperature changes than lithium ones. The biggest disadvantage, currently, is due to lower energy density, which means that EVs with sodium batteries will not be able to travel as far as it is possible with lithium. The main difference between Li and Na ASSBs is in the electrolyte. Increasing the voltage of the sodium batteries causes instability of the electrolyte [161]. The same authors found a novel electrolyte where the utilization of a sodium bis(fluorosulfonyl)imide (NaFSI) salt, known for its enhanced stability, in combination with a solvent possessing a reduced dielectric constant, has been proposed to stabilize the anode at a high-operating-voltage (4.2 V) sodium-ion battery and prolong its cycle life. Additionally, it reduces the solvability of the anode protection layer and, therefore, enables the long-term operation of sodium-ion batteries. Recent progress in solid-state electrolyte materials has been reported in the literature [36,152,162–164].

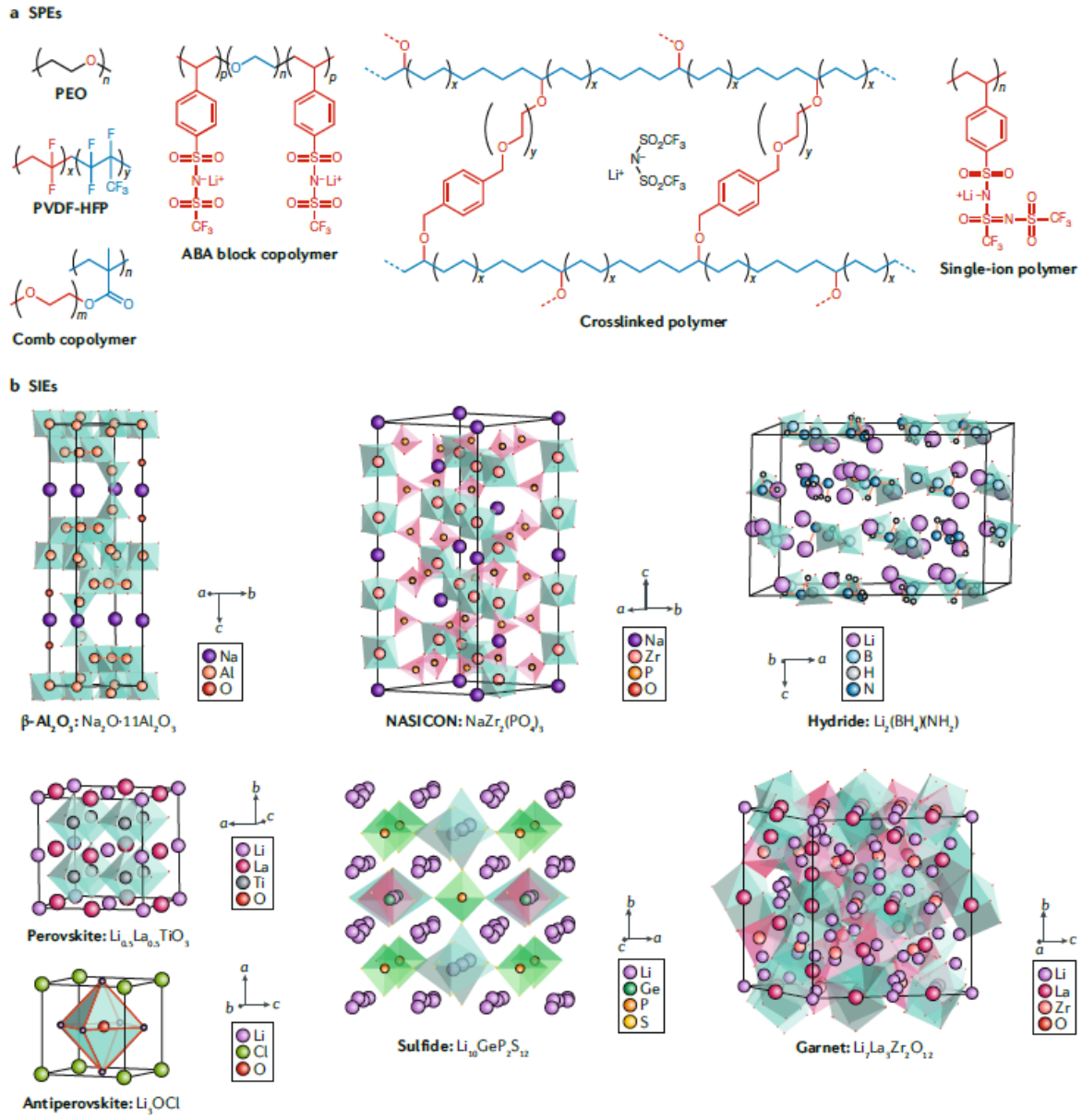

Figure 3. Structures of common solid-state electrolytes: (**a**) solid polymer electrolytes (SPEs) and (**b**) solid inorganic electrolytes (SIEs). Reprinted with permission from [148]. https://www.nature.com/articles/s41578-019-0165-5 (accessed on 20 December 2023). Copyright © 2020, Springer Nature Limited.

Among RT Na-ion conductors, special attention has been recently set on the family of sulfides, which have the advantages of good mechanical strength and mechanical flexibility and low grain-boundary resistance; their disadvantages are sensitivity to moisture, low oxidation stability, and poor compatibility with sodium metal. In the study of Hayashi and co-authors, a sodium-ion conductor, $Na_{2.88}Sb_{0.88}W_{0.12}S_4$, has been reported to exhibit higher conductivity compared to the standard electrolyte, $Li_{10}GeP_2S_{12}$. By partially replacing antimony with tungsten in Na_3SbS_4, sodium vacancies are created, and a tetragonal-to-cubic phase transition occurs. This results in maximum conductivity at room temperature, measuring 32 mS cm^{-1}, for a sintered body with the composition $Na_{2.88}Sb_{0.88}W_{0.12}S_4$. Furthermore, this sulfide has further benefits, such as resistance to moisture and the possibility of becoming denser at significantly lower sintering temperatures compared to standard oxide-based sodium-ion conductors, which require temperatures above 1000 °C [162]. Another interesting class is boron hydrides, which show wide electrochemical stability windows, stability with sodium metal, high thermal and chemical stability, and stability in air. However, they often exhibit large interfacial resistance. $Na_{2-x}(CB_{11}H_{12})_x(B_{12}H_{12})_{1-x}$ shows a fast ionic Na conductivity of 2 mS cm^{-1} at RT, reaching the superionic regime above 60 °C [16,36,123,162,165]. Oxide-based materials, especially NASICON, show great potential as solid electrolytes. NASICON is one of the most promising oxide-based solid electrolytes with suitable 3D tunnels for Na-ion migration, high thermal and chemical stability, high mechanical strength, and very high electrochemical oxidation voltage. Generally, the NASICON term is used to describe a special crystalline structure with the general composition formula AMP_3O_{12}, where the A site can be either vacant or filled to maintain electric neutrality, thus greatly affecting the amount of mobile Na ions as well as the interaction between the mobile Na ions and the immobile skeleton atoms. The first NASICON-type solid electrolyte, $Na_3Zr_2PSi_2O_{12}$, was reported by Goodenough et al. It had a monoclinic structure and showed an ionic conductivity of 2×10^{-1} S cm^{-1} at 300 °C, which is comparable to β''- alumina, another excellent Na-ion conductor [166].

Another very important aspect is the overall compatibility of the cathode, anode, and solid electrolyte. Commonly used cathode materials in ASSBs are metal oxides or sulfides, especially materials based on layer structures. Mixed transition-metal (TM) oxides can deliver specific energy densities close to 600 Whkg^{-1}. The organic cathode material pyrene-4,5,9,10-tetraone (PTO) maintains intimate interfacial contact with the solid electrolyte during cycling, thus improving cycle life with high specific energy (587 Wh kg^{-1}) and record cycling stability (500 cycles) [167]. Therefore, a good solution for the problem related to poor contact with solid electrolytes can be found in the formation of composite materials [168], microstructural control, chemical infiltration, etc. [169,170]. The most common anode materials, similar to those in batteries containing a liquid electrolyte, are Na alloys, hard carbon, expanded graphite (EG), various metal oxides, and, most popularly, Na metal anodes. The Na metal anode, due to its high theoretical capacity (1166 mA h g^{-1}) and low redox potential (−2.71 V vs. the standard hydrogen potential), possesses a higher working voltage and higher energy density than those of Li [139]. Also, the Na metal has a lower melting point and mechanical modulus, providing a highly wettable anode interface. Still, two problems occur with respect to the Na metal anode: dendrite growth and the instability of the interfaces. Although extensive efforts have been made to investigate metal dendrite growth in solid electrolytes, its fundamental understanding is still incomplete [171–173]. Obviously, sodium batteries could become a viable, cheaper alternative to lithium, but it may take several years to reach an adequate level of technology readiness.

Since the first superionic conduction in $LiBH_4$ was reported [174], metal complex hydrides with light weight, high electrochemical stability, and excellent deformation properties [175] have been attracting attention as a potential solid electrolyte material. Consequently, the investigation of superionic conductivity was expanded to include the $[B_{10}H_{10}]^{2-}$ and $[B_{12}H_{12}]^{2-}$ compounds, which are believed to be intermediate products of the dehydrogenation process of $[BH_4]^-$ compounds and are more stable [176–178].

Complex hydrides often demonstrate a characteristic first-order phase transition from a low-temperature phase to a high-temperature phase at a specific temperature. This shift is accompanied by a significant enhancement in conductivity, typically spanning several orders of magnitude [174,176–178]. However, it is important to note that the temperature at which this phase change occurs is typically significantly higher than 373 K, making it unsuitable for practical applications. Several studies reported the use of various electrolytes, such as $Li_xNa_{1-x}B_{12}H_{12}$, $NaCB_{11}H_{12}$, $Na_3BH_4B_{12}H_{12}$, $NaCB_9H_{10}$, and $Na_2B_{10}H_{10}$–$Na_2B_{12}H_{12}$, to enhance conductivity and lower the phase transition temperature [16,62,63,155,179–185].

Another important type of inorganic electrolyte is Mg^{2+}-based solid electrolytes, which exhibit transport characteristics that are intimately related to the crystal structure. When compared to Li-ion technology, Mg-ion batteries (MIBs) have several benefits [186–188]. Mg/Mg^{2+}'s electrochemical potential (vs. a standard hydrogen electrode, or SHE) is 2.4 V, while Li/Li^+'s electrochemical potential is 3.0 V. High cell voltages are, therefore, made possible. Metallic Mg has a greater volumetric capacity (3.833 mAh cm^{-3}) than Li metal (2.036 mAh cm^{-3}). Mg is also harmless and has convenient handling qualities [189,190]. Also, compared to Li (0.006%), it is more prevalent (2%) in the Earth's crust. Dendrites are less frequent in the case of Mg than Li [191,192]. All of the aforementioned factors, along with the metal magnesium's extremely high capacity, position magnesium as a safer and more dependable anode material compared to lithium. A secondary magnesium battery using $Mg(BH_4)_2$ dissolved in tetrahydrofuran (THF) and dimethyl ether (DME), and later $Mg[B(OCH(CF_3)_2]$ in DME, demonstrated a record-high electrochemical stability window of 4.3 V, even in the field of liquid electrolytes. Additional benefits include a high Mg-ion conductivity of $1.1 \cdot 10^{-2}$ S cm^{-1} and stability in air [193,194].

2.2.2. Solid Polymer Electrolytes

When comparing SIEs with SPEs, it becomes evident that SPEs possess various advantages. These advantages encompass the simplicity of synthesis, low mass densities, chemical stability, affordability, compatibility with large-scale production processes, and the mechanical toughness inherent in organic polymers at temperatures significantly surpassing the glass transition point. Hydrocarbon polymers, such as polyethylene and polypropylene, fulfill the above-mentioned attributes, but dielectric constants often exhibit low values. Hence, these materials are incapable of fulfilling the requirement for efficient cationic transport and facilitation of ion-pair dissociation in an electrolyte [138]. Therefore, it is not unexpected that polymers such as poly(ethylene oxide) (PEO), poly(acrylonitrile) (PAN), poly(methyl methacrylate) (PMMA), and poly(vinyl alcohol) (PVA) are commonly used (Figure 3a) [148]. The electron-withdrawing groups dispersed along the carbon–carbon backbones in those materials enable ion-pair dissociation through specific, non-classical effects [195]. The processes that lead to ion-pair dissociation consistently involve the dynamic connection between the mobile cations and the long-chain molecules that make up the solid polymer electrolyte. In contrast to solid electrolytes, where cations exhibit mobility by traversing atomic positions within a crystal lattice or more expediently along lattice defects or grain boundaries, the presence of polymer chains confined within a crystal lattice impedes the movement of cations that are linked to groups along the chain's central structure [138]. Fortunately, there are several physical methods, such as the use of polymer blending, inorganic fillers, plasticizers, and oligomer-tethered nanoparticles, as well as chemical techniques like co-polymerization, cross-linking, and the incorporation of ionic side groups. These approaches can be employed to design solid polymer electrolytes that hinder the crystallization process, thereby facilitating the attainment of desirable levels of ionic conductivities at temperatures close to RT or within a range suitable for various applications, including those in the field of transportation [148,196].

A novel solid polymer electrolyte has been recently developed utilizing PEO as the polymer matrix and LiTFSI and 1-butyl-1-methylpyrrolidinium bis(trifluoromethanesulfonyl)imide (Pyr14TFSI) as the fillers. According to the paper [197], the manipulation of the surface properties of the solid polymer electrolyte has the potential to enhance the interaction with

lithium metal, hence improving the process of lithium electrodeposition and electrodissolution. Furthermore, the utilization of LiTFSI salt was employed in the synthesis of various solid polymer electrolytes consisting of poly(ethyleneglycol)diacrylate (PEGDA) and a succinonitrile plasticizer, resulting in a notable ionic conductivity of approximately 0.43 mS cm^{-1} at ambient temperature. Additionally, UV-photocurable polyurethane acrylate (PUA) containing 30 wt.% LiTFSI exhibited a peak ionic conductivity of 0.0032 mS cm^{-1} at RT. Also, the utilization of ether-based electrolytes that undergo in situ polymerization by a ring-opening process in the presence of aluminum fluoride (AlF_3) exhibits encouraging properties for addressing the existing limitations of oxidative stability and interfacial charge transport in current solid polymer electrolytes.

2.2.3. Composite Solid Electrolytes

Due to the notable advantages of solid inorganic electrolytes and solid polymer electrolytes, the integration of SIE-SPE composites has become a progressively appealing strategy for developing materials with the most favorable characteristics of both their SIE and SPE constituents (Figure 4) [128,138].

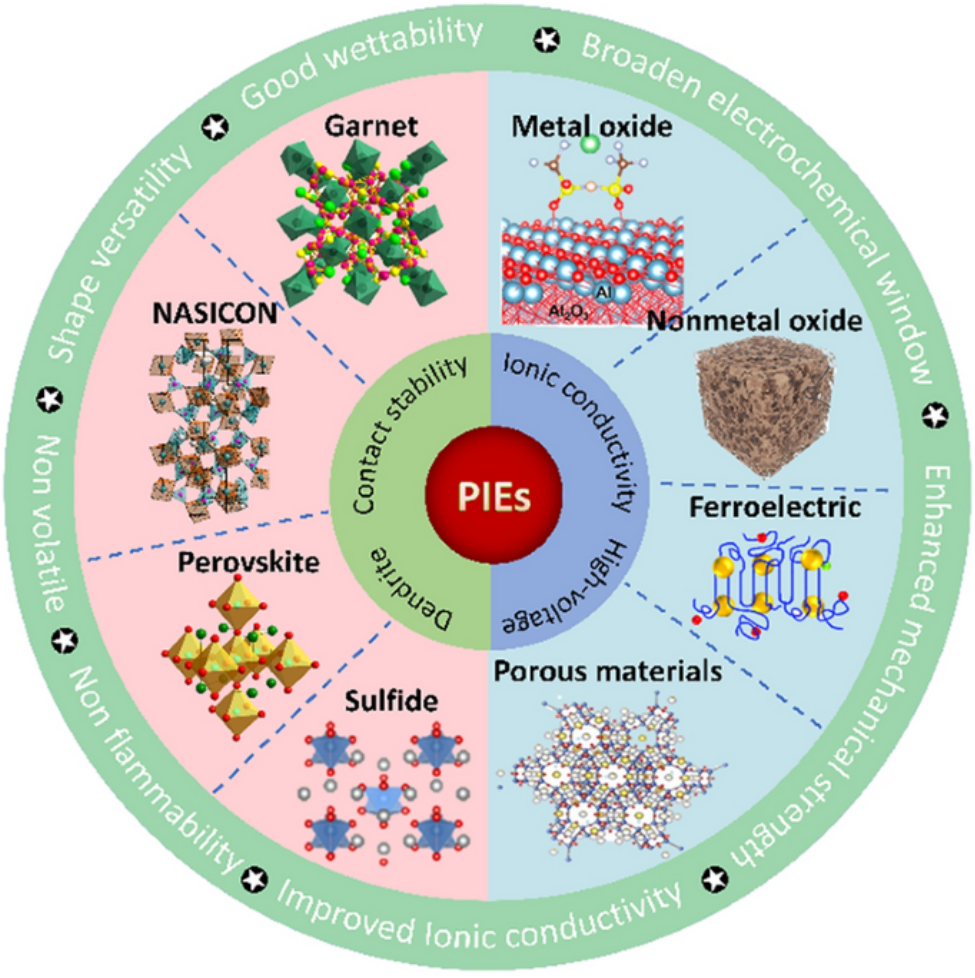

Figure 4. Characteristics of polymer inorganic electrolytes. Reprinted with permission from [128]. https://doi.org/10.1007/s40820-022-00996-1. https://creativecommons.org/licenses/by/4.0/ (accessed on 20 December 2023).

The development of composite electrolytes can be attributed to the inert inorganic particles' incorporation into ion-conductive engineering polymers, such as PEO. This incorporation serves to enhance the mechanical strength and thermal stability of the composite electrolytes while also inhibiting polymer crystallization and promoting greater disso-

ciation of the salt [198]. Furthermore, there have been suggestions that the presence of well-connected channels within the inorganic phase facilitates enhanced ion conduction rates. Also, in addition to bulk composite electrolytes, layered solid polymer electrolytes and solid inorganic electrolyte hybrids demonstrate features that depend on their phase and are particular to their intended use. The task-specific qualities refer to characteristics that can enhance the interaction between an intercalating cathode and an interface or enhance the chemical and/or electrochemical stability of a solid-state electrolyte when in contact with reactive alkali-metal anodes [199].

In the study of Hiraoka and co-authors, flexible and self-supporting CSEs composed of a polyether-based polymer and inorganic $Na_3Zr_2Si_2PO_{12}$ (NZSP) were prepared to harness the combined benefits offered by both materials. The conductivity of CSEs containing 30 wt.% NZSP was high, 1.03×10^{-5} S cm^{-1} at 298 K. After DSC and FT-IR spectroscopy measurements, it was revealed that decreased T_g and the promotion of NaTFSA dissociation induced by the relatively low content of NZSP caused high conductivity. The problem of the interfacial properties of the CSEs with a Na metal negative electrode was solved by adding 200 wt.% of NZSP in the CSE mixture, exhibiting the lowest resistivity and activation energy of all the electrolytes [200].

Another study employed the sol–gel method to initially synthesize nanosized powders of NASICON-type NZSP. Subsequently, a solution-casting technique was employed to produce two types of composite solid electrolytes, including PEO and non-zeolitic silica particles. These electrolytes show remarkable ionic conductivities above 10^{-4} S cm^{-1} at an elevated temperature of 55 °C. Additionally, they exhibit a wide electrochemical window surpassing 4.7 V vs. the Na^+/Na reference electrode, along with the capacity to effectively hinder the formation of sodium dendrites. Sodium ASSBs utilizing the $Na_{0.67}Ni_{0.33}Mn_{0.67}O_2$ cathode and two kinds of flexible polymer/ceramic (PEO-based and NZSP-based) composite solid electrolytes demonstrate remarkable electrochemical characteristics. These include a substantial discharge capacity of 73.2 mA h g^{-1} (68.2 mA h g^{-1}) and an impressive capacity retention rate of 98.4% (97.6%) after undergoing 100 cycles at a temperature of 55 °C and a charging rate of 0.5 C. The findings of this study offer a promising approach to the development of high-performance sodium ASSBs [201].

2.3. Problems with Solid Electrolytes and Possible Solutions

Undoubtedly, there are still several pressing issues that hinder the widespread implementation of ASSBs. One example of a phenomenon observed in high-energy-density solid-state battery systems is significant capacity deterioration, which can be attributed to several electrochemical and mechanical factors [152,202]. Additionally, the power density associated with their high-rate characteristic, specifically their ability to charge and discharge rapidly, is insufficient to meet the requirements of commercial applications [138].

As already mentioned, SE should possess a few characteristics, such as sufficient ion conductivity, low interfacial resistance at ambient temperature, and wide and stable electrochemical windows to accommodate various types of active materials. Additionally, due to the stress induced by thermal cycling or the distortion of electrodes during the charge–discharge process, solid electrolytes should have a large thermal stability window, good mechanical properties, and high conductivity. The problem is that many solid electrolytes only work at high temperatures (HTs) and fail to conduct ions at RT. Although significant efforts are being devoted to improving the ionic conductivity of solid electrolytes [203], characteristics like electronic transport, energy density, and cycling stability of solid-state batteries are less often in focus [21,204]. A recently reported fast and stable solid electrolyte, $Li_8B_{10}S_{19}$, outperforms many other electrolytes in terms of stability. While most of the fast-ion-conducting materials break down quickly, this material shows extraordinary durability. That was confirmed by measurements of an electrochemical window of 1.2 V, a factor of two wider than other fast-conducting sulfide materials. Additionally, a critical current density of 1 mA cm^{-2} was observed with a charge/discharge capac-

ity of 1 mAh cm^{-2}, making this material the most stable fast-Li-ion-conducting sulfide ever reported [205].

Among other issues, the severe instability of the solid electrolyte interphase formed during repeated cycling certainly represents an important factor that hinders the faster development of some ASSBs. This instability of the SEI results in ongoing side reactions, depletion of electrolytes, and irreversible loss of capability, which makes sodium batteries less stable than lithium ones [161]. The occurrence of dendrite growth during extended cycling is a key event that leads to short-circuiting and thermal runaway, hence posing significant safety concerns. Most of these issues are associated with the kinetics of ion diffusion, the interface between the electrode and the electrolyte, and the chemo-mechanical interaction among different components [159].

Due to the rigidity of the cathode and solid electrolyte and the very limited contacting area, the direct contact of these two species leads to poor solid–solid contact at interfaces and consequently high interfacial resistance. NaSICON-structured cathode materials have greater interface compatibility and considerably lower interfacial charge-transfer resistance when compared to other cathode materials. As a result, these materials demonstrate the highest electrochemical performance in ASSBs that are based on sodium superionic conductor-type solid electrolytes. The interfacial resistance can be solved via the formation of composite cathodes because homogeneous distribution and/or reduction in the particle size of the composite electrodes will be obtained, effectively decreasing interfacial resistance [203]. A summary of the electrolyte materials in ASSBs, including ionic conductivities, electrochemical stability, and mechanical properties, is shown in Table 1 [139].

Table 1. Summary of electrolyte materials in ASSBs. Reprinted with permission from [139]. https://doi.org/10.1002/aesr.202000057. https://creativecommons.org/licenses/by/4.0/ (accessed on 20 December 2023).

Type	Materials	Conductivity [S cm^{-1}]	Potential Window (V versus Na^+/Na)	Advantages	Disadvantages
Polymer-based	PEO-Na salt PEG, PVDF-HFP, etc.	10^{-6}–10^{-4}	≈4.5	Stable with sodium metal, lightweight, highly flexible	Low ionic conductivity, limited thermal stability, low oxidation stability
Oxides	N-β″-Al_2O_3 NASICON $Na_2M_2TeO_6$	10^{-4}–10^{-3}	Up to 7	High thermal and chemical stability, high mechanical strength, high electrochemical oxidation voltage	High grain boundary resistance, large interfacial resistance
Sulfides	Na_3PS_4 $Na_{11}Sn_2PS_{12}$ and their derivatives	10^{-4}–10^{-3}	<4 for Na_3PS_4 Others up to 5	Good mechanical strength and mechanical flexibility, low grain-boundary resistance	Sensitive to moisture, low oxidation stability, poor compatibility with sodium metal
Boron hydrides	$Na_{2-x}(B_{12}H_{12})_x(B_{10}H_{10})_{1-x}$ $Na_{2-x}(CB_{11}H_{12})_x(B_{12}H_{12})_{1-x}$ etc.	10^{-4}–10^{-2}	Up to 5	Wide electrochemical stability windows, stability with sodium metal, high thermal and chemical stability, and stability in air	Limited researches, large interfacial resistance

2.4. Mechanochemical Techniques

Mechanochemical techniques offer a viable alternative to solvent-based processes and traditional solid-state synthesis. These approaches enable the mechanochemical synthesis of solid electrolytes and facilitate the processing of cathode composites, even on a large scale. In recent years, there has been a notable growth in the utilization of mechanical milling for the processing of solid electrolytes and solid-state battery composites.

The processing and scaling up of solid-state batteries remain complex tasks. While mechanochemical synthesis shows promise in facilitating the scaling-up process, there is still a lack of comprehensive understanding of its impact on the various compounds involved. The fabrication of solid electrolytes for their application as separators to improve the interface behavior between the anode and the electrolyte presents one of the most significant challenges. Similarly, the production of cathode composites is also a complex task, as it involves multiple phases (such as the cathode active material, solid electrolyte, carbon

additives, and binders) that exhibit distinct behaviors during processing. Mechanochemical methods have been used for the synthesis or modification of a whole group of solid electrolytes and complex hydrides that show high levels of ionic conductivity [1,206–208]. The preparation of solid electrolytes as well as composites by milling procedures has usually been approached in a rather phenomenological manner, mostly as a trial-and-error method. Recent research has demonstrated the significant impact of milling parameters and mechanochemical synthesis on the structure and transport properties of ionic conductors and composite electrodes. Furthermore, these factors also affect the performance of solid-state batteries [209–215].

As an example of the synthesis of solid-state electrolytes, Rao and co-authors reported the first RT all-solid-state Na-Se battery prepared by using the fast-ion-conducting mechanochemically synthesized $Na_{11}Sn_2PSe_{12}$ (NSPSe). The highest RT bulk ionic conductivity of the mechanochemically synthesized NSPSe was 1.0 mS cm^{-1}. The use of this fast-ion-conducting material enabled the successful demonstration of the first Na-Se all-solid-state batteries, namely $Na/Na_{11}Sn_2PSe_{12}$/C-Se and $Na_3Sn/Na_{11}Sn_2PSe_{12}$/C-Se. These batteries exhibited specific initial discharge capacities of 430 mA h g^{-1} and 400 mA h g^{-1}, respectively, when operated at a current density of 0.08 mA cm^{-2}. The $Na_3Sn/Na_{11}Sn_2PSe_{12}$/C-Se battery demonstrated a cycling capability of 500 cycles, wherein the capacity steadily fell to 50 mA h g^{-1} [216].

Also, Molaiyan and Witter prepared $Sm_{1-x}Ca_xF_{3-x}$ ($0 \leq x \leq 0.15$) solid-state electrolytes via solid synthesis: high-energy ball milling, a straight-forward preparation method that does not demand any pretreatment, providing a scalable and flexible option for battery applications [217–219]. The fluoride ionic conductivities of these materials at RT are in the range of 10^{-5}–10^{-6} S cm^{-1}; therefore, they can be used for fluoride shuttle applications as a candidate for secondary fluoride ion battery applications. Based on the achieved conductivity of the $Sm_{0.95}Ca_{0.05}F_{2.95}$ solid-state electrolyte, an electrochemical cell on well-known electrodes, $CeF_3/Sm_{0.95}Ca_{0.05}F_{2.95}$/Bi, has been tested. Bi was chosen as the cathode material because of its high ionic conductivity for fluoride at RT. The electrochemical cell in the study underwent charging and discharging processes with a current density of 1 μA cm^{-2} at a temperature of 75 °C, within a voltage range of 0.01 to 0.90 volts (with a theoretical voltage of 2.8 volts) [220].

In the study of Yamanaka and co-authors, the $MgS–P_2S_5–MgI_2$ glasses and glass-ceramics were prepared by mechanochemical synthesis followed by heat treatment in order to obtain sulfide solid electrolytes with high Mg^{2+}-ion conductivity. The formula used was $(100 - x)(0.6MgS{\cdot}0.4P_2S_5) \cdot xMgI_2$ ($0 \leq x \leq 30$), which includes $P_2S_6^{4-}$ ions. An increase in MgI_2 content induced an increase in conductivities. The highest conductivity of 2.1×10^{-7} S cm^{-1} at 200 °C was obtained for samples with composition x = 20 [221].

Although the above-mentioned protocols are mostly solvent-free, an example of the solvent-assisted approach during ball mill processing was reported in the research of Song et al. [222]. A garnet solid electrolyte, $Li_{6.4}Al_{0.233}La_3Zr_{1.95}Ca_{0.05}O_{12}$, was prepared by mechanochemical milling of Li_2CO_3, La_2O_3, and $Zr_{1.95}Ca_{0.05}O_{3.95}$ in ethanol, with a subsequent crystallization step. The resulting ionic conductivity was high, at 0.52 mS cm^{-1}. The formation of a liquid buffer layer during the process of ball milling not only impacts the microstructure but also substantially influences the energy transfer to the precursors. The utilization of solution-assisted milling has limitations due to the issues of chemical reactivity between solid electrolytes and certain solvents [223].

Several studies were conducted to elucidate the significance of anion dynamics in the process of cation diffusion in different complex hydrides that exhibit ionic conductivity at a magnitude of approximately 1 mS cm^{-1}. Different novel hydroborate solid electrolytes have been effectively evaluated in electrochemical cells to date [58,224–228]. The comparative analysis of hydroborates, phosphates, and oxides reveals that the low gravimetric density exhibited by hydroborates highlights their potential as a viable option for enhancing cell energy density, especially in the family of closodeca- and dodeca-hydroborates. The series of sodium-based compounds is obtained through the combination of the Na-based closo-

and carbacloso-hydroborates, namely $NaCB_9H_{10}$, $Na_2B_{10}H_{10}$, $NaCB_{11}H_{12}$, and $Na_2B_{12}H_{12}$, by the mechanochemical synthesis in planetary or vibrational mills (Figure 5) [20,229]. The electrochemical stability of the compounds was proven, and an oxidation range of 3 to 4 V vs. Na^+/Na was identified, which varied depending on the selected anion pair. The electrochemical oxidation of each mixed phase is governed by the stability of the single anion with the lowest stability toward oxidation. Thus, by arranging all anions based on their maximum oxidation potential, it can be inferred that [CB_9-B_{10}] is the least stable mixture and [CB_{11}-B_{12}] is the most stable [229].

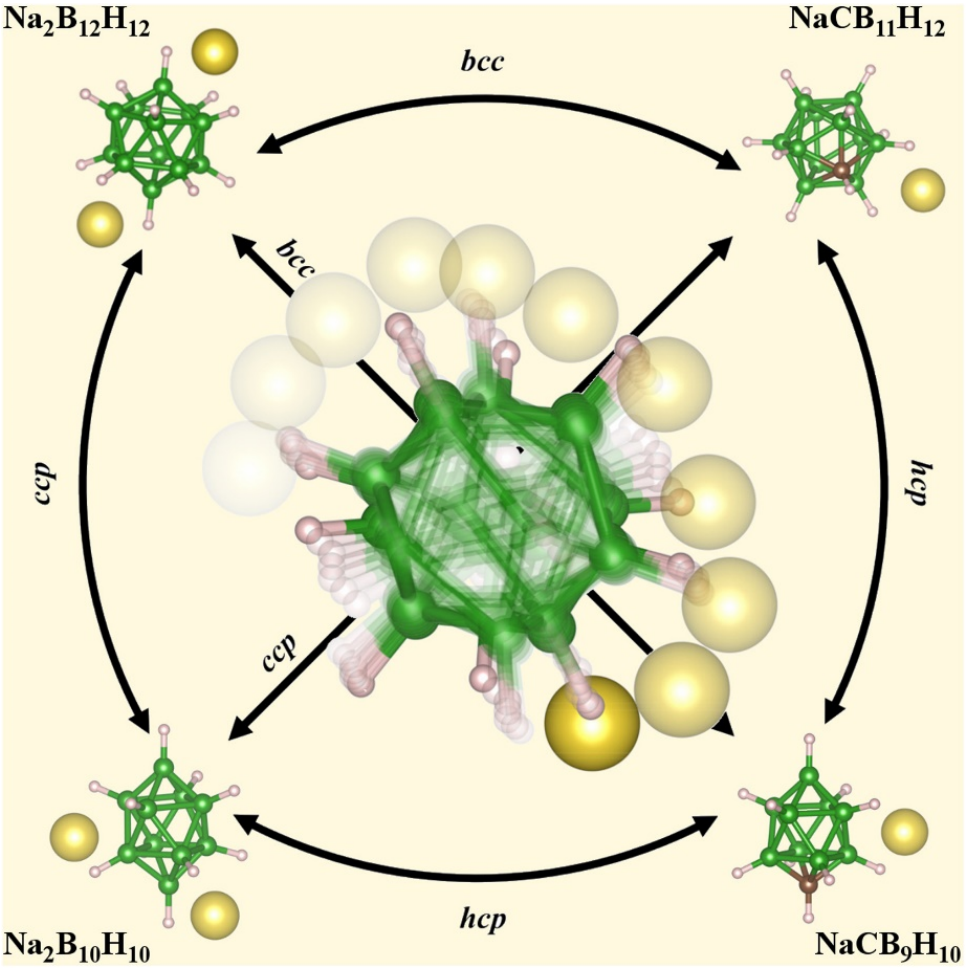

Figure 5. Binary mixtures of *closo*-hydroborate sodium salts. Reprinted with permission from [20]. https://doi.org/10.1016/j.jallcom.2021.162659. https://creativecommons.org/licenses/by-nc-nd/4.0/ (accessed on 20 December 2023).

Metal dodecaborates $M_{2/n}B_{12}H_{12}$, where n represents the valence of the metal M, have garnered growing attention as promising energy materials, particularly in the fields of hydrogen storage and superionic conductivity. A unique method for synthesizing anhydrous $M_{2/n}B_{12}H_{12}$ (where M represents Li, Na, and K) without the use of solvents has been established [178]. The thermal stability and transformations of the anhydrous single-phase $Li_2B_{12}H_{12}$ indicate the potential formation of the high-temperature polymorph of $Li_2B_{12}H_{12}$ during the dehydrogenation process of $LiBH_4$. This highlights the need for additional research into the decomposition mechanism of metal borohydrides and metal dodecaborates [178,230–241].

The exceptional stability exhibited by the icosahedral $[B_{12}H_{12}]^{2-}$ structure lends itself to possible use as a solid electrolyte. In a recent study, the Na^+ conductivity of $Na_2B_{12}H_{12}$ was found to be 0.1 S cm^{-1} above the order–disorder phase transition at around 529 K.

This value is comparable to the Na^+ conductivity of a polycrystalline β″-Al_2O_3 solid-state Na electrolyte, which is 0.24 S cm^{-1} at 573 K [179,232,242]. $Na_{2-x}(CB_{11}H_{12})_x(B_{12}H_{12})_{1-x}$ showed a fast ionic Na conductivity of 2 mS cm^{-1} at room temperature. Additionally, it possesses a low activation energy of 314 meV in a thermodynamically and electrochemically stable structure, which explains why it can be potentially used as a solid electrolyte in future Na-ASSBs. Cyclic voltammetry measurements with a specialized setup for solid-state electrolytes demonstrated a wide operating window (up to 4.1 V vs. Na^+/Na) [232].

To enhance the ionic conductivity of $M_{2/n}B_{12}H_{12}$, it was proposed that an additional metal enabling the formation of bimetallic dodecaborate compounds should be introduced. It was theorized that the presence of two different metallic elements in the compound might potentially result in a synergistic effect, leading to a greater change in ion mobility [243–246].

A study by He and co-authors reports the bimetallic dodecaborate compound $LiNaB_{12}H_{12}$ prepared via the mechanochemical reaction of $LiBH_4$, $NaBH_4$, and $B_{10}H_{14}$ with a stoichiometric molar ratio of 1:1:1. Notably, $LiNaB_{12}H_{12}$ exhibits a lower phase transition temperature (488 K) compared to its individual counterparts, $Li_2B_{12}H_{12}$ (615 K) and $Na_2B_{12}H_{12}$ (529 K), as previously reported. Furthermore, the ionic conductivity of $LiNaB_{12}H_{12}$ reaches a noteworthy value of 0.79 S cm^{-1} at 550 K. The conductivity value is roughly eight times greater than that of $Na_2B_{12}H_{12}$ and eleven times greater than that of $Li_2B_{12}H_{12}$ [179].

Beside sodium and lithium, magnesium borohydride chemistry also represents an important playing field while questing for new solid-state electrolytes [247,248]. Roedern et al. mechanochemically prepared a new compound, $Mg(en)_1(BH_4)_2$, starting with $Mg(BH_4)_2$ and ethylenediamine ($H_2N(CH_2)_2NH_2$), which, at the time, had the greatest documented Mg-ion conductivity (up to $6{\cdot}10^{-5}$ S cm^{-1} at 343 K). Mechanochemical milling procedures alone were used in the synthesis, which was then subjected to an extra heat treatment. Additionally, a mixture with diglyme has reported conductivities of 2×10^{-5} S cm^{-1} at 350 K for $Mg(diglyme)_{0.5}(BH_4)_2$, along with other solvated derivatives of the $Mg(BH_4)_2$ precursor [247,248]. $Mg(NH_2)(BH_4)$ is another good solid-state Mg-ion conductor, with its electrochemical window estimated to be approximately 3 V using cyclic voltammetry [249]. Furthermore, $Mg_3(NH_2)_2(BH_4)_4$ exhibits a reported conductivity of 4×10^{-5} S cm^{-1} at 373 K [250]. Jensen et al. recently released a ground-breaking paper in which they reported a conductivity of $Mg(BH_4)_2NH_3$ amounting to $3.3{\cdot}10^{-4}$ S cm^{-1} at 353 K [251]. They proposed a new mechanism based on NH_3 dynamics to explain the conductivity in these materials [252]. It was also found that $Mg(BH_4)_{22}NH_3BH_3$ and other analogous materials exhibit high conductivity in the range of 10^{-4} S cm^{-1} [253–255]. Other good conductors based on M-B-N-H (M = Li, Mg) systems have also been reported [251,256–259].

Ball milling has also been well recognized as a means of introducing defects that are considered advantageous for enhancing ion conductivity in many solid electrolytes. Promoting perturbation in solid crystals is a widely recognized approach that serves to stabilize non-equilibrium phases in diverse materials or facilitate the formation of structural flaws [127,260].

In their study, Murgia et al. documented the successful stability of the body-centered cubic (bcc) polymorph of $NaCB_{11}H_{12}$ (NCB) at RT through the utilization of high-energy mechanical milling, achieving this outcome within a mere 15 min duration. As anticipated, the conductivity of Na ions exhibited a consistent increase throughout the milling process, culminating in a peak value of 4 mS cm^{-1} at RT after 45 min (Figure 6). Surprisingly, conducting additional mechanical grinding for a duration of up to 2 h resulted in a reduction in conductivity. Furthermore, extending the milling process to 6 h resulted in a substantial decrease in the conductivity of sodium ions (measured at 9.78×10^{-9} S cm^{-1} at RT), accompanied by a considerable decrease in crystallinity. The observed increase in Na-ion conductivity after a 45 min milling process can be attributed to the stabilization of the body-centered cubic polymorph at RT. The bcc structure has a less effective arrangement of anions compared to the orthorhombic starting structure, but it offers improved and wider

conduction pathways for Na^+ ions due to a reduced diffusion distance. Nevertheless, the underlying cause for the decline in conductivity beyond milling durations of over 45 min has not been thoroughly examined [261].

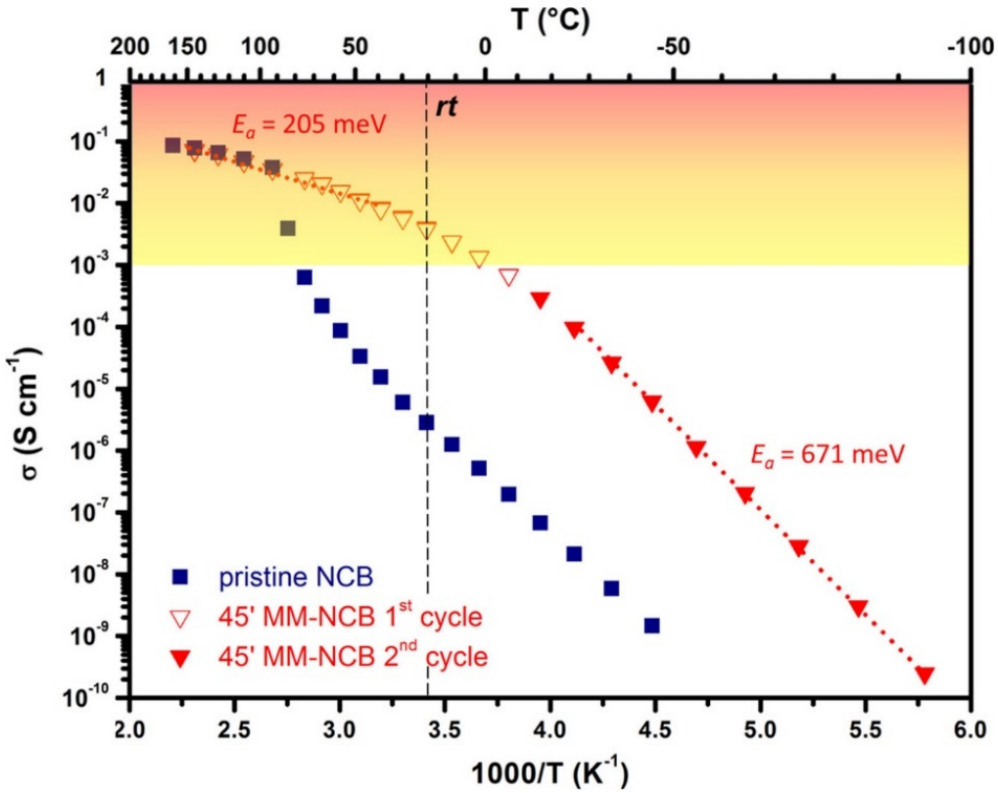

Figure 6. The conductivity of a sample mechanically milled for 45 min is 4 orders of magnitude larger than that of a pristine sample. Reprinted with permission from [261]. https://doi.org/10.1021/acsami.1c21113 (accessed on 20 December 2023). Copyright © 2021, American Chemical Society.

Finally, it is important to highlight that mechanochemical synthesis allows the achievement of kinetic control, which stands in contrast to the conventional high-temperature solid-state synthesis that is thermodynamically regulated. As a result, mechanochemical synthesis enables the preparation of materials that are thermodynamically less stable [1]. For example, Li_2ZnCl_4 can exist in two distinct polymorph types that are challenging to separate. The solid-state synthesis conducted at high temperatures primarily results in the formation of a metastable olivine-type structure, alongside the co-existence of a spinel-type structure at lower temperatures. One potential method for obtaining pure spinel involves subjecting the combination to an annealing process at low temperatures for several weeks. In contrast, when prepared via a mechanochemical method, the single product formed is the low-temperature spinel-type modification, and this occurs within a relatively short period throughout the synthesis process. The reaction pathways involving heating in the ampoule and momentum transfer in the mill exhibit distinct characteristics, leading to the potential formation of different polymorphs with different electrochemical characteristics [262].

Another example of how the use of mechanochemical synthesis, i.e., kinetic energy transfer, allows metastable compounds and local structures not obtainable via classic solid-state routes to be formed was reported in the work of Zhao et al., where the beneficial effect of an aliovalent substitution on Li_3PS_4 was observed. A mixture of the precursors P_2S_5, Li_2S, and ZnO was pre-processed via milling and subsequently crystallized, which resulted in the successful co-incorporation of Zn^{2+} and O^{2-}, increasing the ionic conductivity of $Li_{3.06}P_{0.98}Zn_{0.02}S_{3.98}O_{0.02}$ up to 1.12 mS cm^{-1} [263].

A comparison of the solid electrolytes and their ionic conductivities is given in Table 2.

Table 2. Comparison of the solid electrolytes and their ionic conductivities.

Solid Electrolyte	Ionic Conductivity (mS cm^{-1})	Reference
LISICON $Li_{14}Zn(GeO_4)_4$	125 (300 °C)	[153]
$LiZr_2(PO_4)_3$	12 (300 °C)	[264]
LiPON	0.002	[154]
$Na_{2.88}Sb_{0.88}W_{0.12}S_4$	32	[162]
$Na_{2-x}(CB_{11}H_{12})_x(B_{12}H_{12})_{1-x}$	2	[16]
$Li_7P_3S_{11}$	45.66	[23]
$Na_7P_3S_{11}$	10.97	[23]
NASICON $Na_3Zr_2PSi_2O_{12}$	200 (300 °C)	[166]
$MgZr_4(PO_4)_6$	6.1 (800 °C)	[265]
ZnZr4(PO4)6	3.7 (800 °C)	[265]
Composite of LiTFSI/PEGDA/succinonitrile plasticizer	0.43	[197]
Composite of polyether-based polymer/inorganic $Na_3Zr_2Si_2PO_{12}$ (NZSP)	0.01	[200]
$Na_{11}Sn_2PSe_{12}$ (NSPSe)	1	[216]
$Sm_{1-x}Ca_xF_{3-x}$ ($0 \leq x \leq 0.15$)	0.01–0.001	[217]
$(100-x)(0.6MgS{\cdot}0.4P_2S_5) \cdot xMgI_2$ ($0 \leq x \leq 30$)	0.00021 (200 °C)	[221]
MgS-P_2S_5-MgI_2	0.00021	[221]
Garnet $Li_{6.4}Al_{0.233}La_3Zr_{1.95}Ca_{0.05}O_{12}$	0.52	[223]
$Na_2B_{12}H_{12}$	0.0001	[179]
β″-Al_2O	0.00024 (300 °C)	[179]
$LiNaB_{12}H_{12}$	0.00079 (280 °C)	[179]
$Mg(en)_1(BH_4)$	0.06 (70 °C)	[249]
$Mg(diglyme)_{0.5}(BH_4)_2$	0.02 (70 °C)	[247]
$Mg_3(NH_2)_2(BH_4)_4$	0.04 (100 °C)	[250]
$Mg(BH_4)_2NH_3$	0.33 (70 °C)	[251]
$Mg(BH_4)_{22}NH_3BH_3$	0.1	[253]
$NaCB_{11}H_{12}$ (NCB) as-prepared	4	[256]
$NaCB_{11}H_{12}$ (NCB) milled	0.00000978	[261]
$Li_{3.06}P_{0.98}Zn_{0.02}S_{3.98}O_{0.02}$	1.12	[263]
$Li_2(BH_4)(NH_2)$	0.2	[107]
$Na_2(BH_4)(NH_2)$	0.003	[266]
$Mg(BH_4)(NH_2)$	0.003 (100 °C)	[250]
LiTFSI-PEO	0.8 (70 °C)	[267]
$LiClO_4$-PEO	0.2–1 (90 °C)	[268]
NaTFSI-PEO	0.15 (70 °C)	[269]
$NaClO_4$-PEO	0.14 (90 °C)	[270]
$LiClO_4$-PEO	0.5 (90 °C)	[270]

3. Conclusions and Perspectives

This paper offers a comprehensive review of the mechanical and physical aspects of milling operations and their impact on the preparation of solid electrolytes, cathode composites, and other materials used in solid-state batteries. It can be seen that numerous

aspects play a significant role, including stressing energy, collision frequency, overall power, particular energy input, and processing time. In conclusion, mechanochemistry can be used as an efficient way for the preparation of all types of SEs, but it also stands out in terms of overcoming the chemical and mechanical stability issues of solid-state batteries. Firstly, this refers to the instability and chemical reactivity of some compounds with solvents; therefore, solvent-free mechanochemical reactions can provide a very important alternative. Additionally, many metastable compounds that cannot be prepared by the standard chemical routes are often achievable by the mechanochemical approach. The incorporation of defects and distortions during the process of mechanochemical milling frequently leads to improved electrochemical performance. The observed phenomenon can be attributed, to a certain degree, to the fragmentation of particles, which leads to improved compressibility and consolidation behavior. Additionally, it may arise from the formation of metastable products and the presence of very faulty material structures. Nevertheless, a noticeable amorphization occurs during the processing of rapid ionic conductors to create composites or separators. Given the potential negative impact on electrochemical performance, more investigation and evaluation of the postprocessing techniques for fast conductors is warranted.

The most important question raised at the end can be summarized as follows: Is there a solid-state electrolyte that fulfills the expectations of safe energy storage systems? Unfortunately, the answer is still negative because some of the issues remain unsolved. Understanding and implementing the interfaces between electrodes and SSEs is a hard task, but in situ and *operando* techniques could be solutions for revealing the answers. To minimize interfacial resistance, it is essential to have close physical contact. Numerous methodologies, particularly those centered on nanotechnology, have effectively mitigated the contact challenges that arise between metal electrodes and solid electrolytes. Nevertheless, the repetitive plating and stripping processes on the anode side unavoidably result in volumetric variations, which subsequently lead to deteriorated contact and increased resistance. Recent findings regarding the incorporation of targeted metals into structurally robust host materials have the potential to provide valuable insights into addressing the challenges. The utilization of a bendable polymer interlayer can also provide an optimal interface between solid materials. Regrettably, electrolytes based on polymers exhibit a diminished level of conductivity when subjected to RT conditions and, on occasion, demonstrate instability and flammability. Hence, achieving a harmonious equilibrium between safety, thickness, and conductivity emerges as the pivotal aspect.

All-solid-state batteries are undoubtedly going to generate a considerable impact in the future. According to projections by the European Commission, it is anticipated that the number of EVs may see a substantial increase, reaching approximately 200 million by the year 2028 and a staggering 900 million by 2040, while the large-scale production of batteries and intensive research could reduce prices by as much as 70 percent. Nevertheless, despite significant advancements in the field of solid-state electrolytes, there is currently a lack of commercially viable ASSBs that can adequately address the increasing needs of today's society.

Author Contributions: Conceptualization, S.B.; writing—original draft preparation, S.B.; writing—review and editing, J.P. All authors have read and agreed to the published version of the manuscript.

Funding: This research received no external funding.

Conflicts of Interest: The authors declare no conflicts of interest.

Abbreviations

Abbreviation	Definition
LiB	lithium-ion batterie
EV	electrical vehicle
NMC	Lithium nickel manganese cobalt oxide
Nb-NCA93	$Li[Ni_{0.92}Co_{0.06}Al_{0.01}Nb_{0.01}]O_2$
PEDOT	poly(3,4-ethylenedioxythiophene)
PSS	poly(styrenesulfonate)
ASSB	all-solid-state battery
SE	solid electrolyte
SSE	solid-state electrolyte
RT	room temperature
SIE	solid inorganic electrolyte
SPE	solid polymer electrolyte
CSE	composite solid electrolyte
LISICON	lithium super ionic conductor
LiPON	lithium phosphorus oxynitride
NASICON	sodium super ionic conductor
NaFSI	sodium bis(fluorosulfonyl)imide
TM	transition metal
PTO	pyrene-4,5,9,10-tetraone
EG	expanded graphite
MIB	Mg-ion battery
THF	tetrahydrofuran
DME	dimethyl ether
PEO	poly(ethylene oxide)
PAN	poly(acrylonitrile)
PMMA	poly(methyl methacrylate)
PVA	poly(vinyl alcohol)
LiTFSI	Lithium bis(trifluoromethanesulfonyl)imide
Pyr14TFSI	1-butyl-1-methylpyrrolidinium bis(trifluoromethanesulfonyl)imide
PEGDA	poly(ethyleneglycol)diacrylate
PUA	polyurethane acrylate
AlF_3	aluminum fluoride
NZSP	$Na_3Zr_2Si_2PO_{12}$
NATFSA	sodium bis(trifluoromethanesulfonyl)amide
HT	high temperature
NSPSe	$Na_{11}Sn_2PSe_{12}$
NCB	$NaCB_{11}H_{12}$

References

1. Schlem, R.; Burmeister, C.F.; Michalowski, P.; Ohno, S.; Dewald, G.F.; Kwade, A.; Zeier, W.G. Energy Storage Materials for Solid-State Batteries: Design by Mechanochemistry. *Adv. Energy Mater.* **2021**, *11*, 2101022. [CrossRef]
2. Quartarone, E.; Mustarelli, P. Electrolytes for Solid-State Lithium Rechargeable Batteries: Recent Advances and Perspectives. *Chem. Soc. Rev.* **2011**, *40*, 2525. [CrossRef]
3. Battery2030+—Battery 2030+. Available online: https://battery2030.eu/ (accessed on 10 November 2023).
4. Anuradha. Understanding Self-Discharge of a Lithium-Ion Battery. EVreporter. Available online: https://evreporter.com/understanding-self-discharge-of-a-lithium-ion-battery (accessed on 10 November 2023).
5. Fast-Charge Lithium Batteries for Electric Vehicles | Flash Battery. Available online: https://www.flashbattery.tech/en/lithium-batteries-electric-vehicles (accessed on 10 November 2023).
6. Boll, C. How Long Do Lithium-Ion Batteries Last? Available online: https://www.protoolreviews.com/how-long-do-lithium-ion-batteries-last (accessed on 11 November 2023).
7. Li, Q.; Yang, Y.; Yu, X.; Li, H. A 700 Wh Kg^{-1} Rechargeable Pouch Type Lithium Battery. *Chin. Phys. Lett.* **2023**, *40*, 048201. [CrossRef]
8. Khan, F.M.N.U.; Rasul, M.G.; Sayem, A.S.M.; Mandal, N. Maximizing Energy Density of Lithium-Ion Batteries for Electric Vehicles: A Critical Review. *Energy Rep.* **2023**, *9*, 11–21. [CrossRef]
9. Divakaran, A.M.; Minakshi, M.; Bahri, P.A.; Paul, S.; Kumari, P.; Divakaran, A.M.; Manjunatha, K.N. Rational Design on Materials for Developing next Generation Lithium-Ion Secondary Battery. *Prog. Solid State Chem.* **2021**, *62*, 100298. [CrossRef]

10. Kim, U.-H.; Lee, S.-B.; Park, N.-Y.; Kim, S.J.; Yoon, C.S.; Sun, Y.-K. High-Energy-Density Li-Ion Battery Reaching Full Charge in 12 min. *ACS Energy Lett.* **2022**, *7*, 3880–3888. [CrossRef]
11. Sun, Q.; Bijelić, M.; Djurišić, A.B.; Suchomski, C.; Liu, X.; Xie, M.; Ng, A.M.C.; Kong Li, H.; Shih, K.; Burazer, S.; et al. Graphene-Oxide-Wrapped $ZnMn_2O_4$ as a High Performance Lithium-Ion Battery Anode. *Nanotechnology* **2017**, *28*, 455401. [CrossRef] [PubMed]
12. Bijelić, M.; Liu, X.; Sun, Q.; Djurišić, A.B.; Xie, M.H.; Ng, A.M.C.; Suchomski, C.; Djerdj, I.; Skoko, Ž.; Popović, J. Long Cycle Life of $CoMn_2O_4$ Lithium Ion Battery Anodes with High Crystallinity. *J. Mater. Chem. A* **2015**, *3*, 14759–14767. [CrossRef]
13. Arbizzani, C.; Gabrielli, G.; Mastragostino, M. Thermal Stability and Flammability of Electrolytes for Lithium-Ion Batteries. *J. Power Sources* **2011**, *196*, 4801–4805. [CrossRef]
14. Li, W.; Xu, H.; Zhang, H.; Wei, F.; Huang, L.; Ke, S.; Fu, J.; Jing, C.; Cheng, J.; Liu, S. Tuning Electron Delocalization of Hydrogen-Bonded Organic Framework Cathode for High-Performance Zinc-Organic Batteries. *Nat. Commun.* **2023**, *14*, 5235. [CrossRef] [PubMed]
15. Wei, F.; Xu, H.; Zhang, T.; Li, W.; Huang, L.; Peng, Y.; Guo, H.; Wang, Y.; Guan, S.; Fu, J.; et al. Mesoporous Poly(3,4-Ethylenedioxythiophene):Poly(Styrenesulfonate) as Efficient Iodine Host for High-Performance Zinc–Iodine Batteries. *ACS Nano* **2023**, *17*, 20643–20653. [CrossRef] [PubMed]
16. Golub, I.E.; Heere, M.; Gounaris, V.; Li, X.; Steenhaut, T.; Wang, J.; Robeyns, K.; Li, H.-W.; Dovgaliuk, I.; Ikeda, K.; et al. Structural Insight into the Magnesium Borohydride—Ethylenediamine Solid-State Mg-Ion Electrolyte System. *Dalton Trans.* **2023**, *52*, 2404–2411. [CrossRef] [PubMed]
17. Janek, J.; Zeier, W.G. A Solid Future for Battery Development. *Nat. Energy* **2016**, *1*, 16141. [CrossRef]
18. Tan, D.H.S.; Banerjee, A.; Chen, Z.; Meng, Y.S. From Nanoscale Interface Characterization to Sustainable Energy Storage Using All-Solid-State Batteries. *Nat. Nanotechnol.* **2020**, *15*, 170–180, Correction in *Nat. Nanotechnol.* **2021**, *16*, 479. [CrossRef]
19. Tian, Y.; Zeng, G.; Rutt, A.; Shi, T.; Kim, H.; Wang, J.; Koettgen, J.; Sun, Y.; Ouyang, B.; Chen, T.; et al. Promises and Challenges of Next-Generation "Beyond Li-Ion" Batteries for Electric Vehicles and Grid Decarbonization. *Chem. Rev.* **2020**, *121*, 1623–1669. [CrossRef]
20. Černý, R.; Murgia, F.; Brighi, M. Metal Hydroborates: From Hydrogen Stores to Solid Electrolytes. *J. Alloys Compd.* **2022**, *895*, 162659. [CrossRef]
21. Shao, B.; Huang, Y.; Han, F. Electronic Conductivity of Lithium Solid Electrolytes. *Adv. Energy Mater.* **2023**, *13*, 2204098. [CrossRef]
22. Sadikin, Y.; Schouwink, P.; Brighi, M.; Łodziana, Z.; Černý, R. Modified Anion Packing of $Na_2B_{12}H_{12}$ in Close to Room Temperature Superionic Conductors. *Inorg. Chem.* **2017**, *56*, 5006–5016. [CrossRef]
23. Richards, W.D.; Tsujimura, T.; Miara, L.J.; Wang, Y.; Kim, J.C.; Ong, S.P.; Uechi, I.; Suzuki, N.; Ceder, G. Design and Synthesis of the Superionic Conductor $Na_{10}SnP_2S_{12}$. *Nat. Commun.* **2016**, *7*, 11009. [CrossRef]
24. Zhou, D.; Shanmukaraj, D.; Tkacheva, A.; Armand, M.; Wang, G. Polymer Electrolytes for Lithium-Based Batteries: Advances and Prospects. *Chem* **2019**, *5*, 2326–2352. [CrossRef]
25. Zhang, H.; Li, C.; Piszcz, M.; Coya, E.; Rojo, T.; Rodriguez-Martinez, L.M.; Armand, M.; Zhou, Z. Single Lithium-Ion Conducting Solid Polymer Electrolytes: Advances and Perspectives. *Chem. Soc. Rev.* **2017**, *46*, 797–815. [CrossRef]
26. Yue, L.; Ma, J.; Zhang, J.; Zhao, J.; Dong, S.; Liu, Z.; Cui, G.; Chen, L. All Solid-State Polymer Electrolytes for High-Performance Lithium Ion Batteries. *Energy Storage Mater.* **2016**, *5*, 139–164. [CrossRef]
27. Yu, Q.; Jiang, K.; Yu, C.; Chen, X.; Zhang, C.; Yao, Y.; Jiang, B.; Long, H. Recent Progress of Composite Solid Polymer Electrolytes for All-Solid-State Lithium Metal Batteries. *Chin. Chem. Lett.* **2021**, *32*, 2659–2678. [CrossRef]
28. Zhao, X.; Wang, C.; Liu, H.; Liang, Y.; Fan, L. A Review of Polymer-based Solid-State Electrolytes for Lithium-Metal Batteries: Structure, Kinetic, Interface Stability, and Application. *Batter. Supercaps* **2023**, *6*, e202200502; Correction in *Batter. Supercaps* **2023**, *6*, e202300177. [CrossRef]
29. Yao, P.; Yu, H.; Ding, Z.; Liu, Y.; Lu, J.; Lavorgna, M.; Wu, J.; Liu, X. Review on Polymer-Based Composite Electrolytes for Lithium Batteries. *Front. Chem.* **2019**, *7*, 522. [CrossRef] [PubMed]
30. Feng, J.; Wang, L.; Chen, Y.; Wang, P.; Zhang, H.; He, X. PEO Based Polymer-Ceramic Hybrid Solid Electrolytes: A Review. *Nano Converg.* **2021**, *8*, 2. [CrossRef] [PubMed]
31. Reinoso, D.M.; Frechero, M.A. Strategies for Rational Design of Polymer-Based Solid Electrolytes for Advanced Lithium Energy Storage Applications. *Energy Storage Mater.* **2022**, *52*, 430–464. [CrossRef]
32. Choudhury, S.; Stalin, S.; Vu, D.; Warren, A.; Deng, Y.; Biswal, P.; Archer, L.A. Solid-State Polymer Electrolytes for High-Performance Lithium Metal Batteries. *Nat. Commun.* **2019**, *10*, 4398. [CrossRef] [PubMed]
33. Popovic, J. Dry Polymer Electrolyte Concepts for Solid-State Batteries. *Macromol. Chem. Phys.* **2021**, *223*, 2100344. [CrossRef]
34. Thangadurai, V.; Narayanan, S.; Pinzaru, D. Garnet-Type Solid-State Fast Li Ion Conductors for Li Batteries: Critical Review. *Chem. Soc. Rev.* **2014**, *43*, 4714. [CrossRef] [PubMed]
35. Jia, M.; Zhao, N.; Huo, H.; Guo, X. Comprehensive Investigation into Garnet Electrolytes toward Application-Oriented Solid Lithium Batteries. *Electrochem. Energy Rev.* **2020**, *3*, 656–689. [CrossRef]
36. Wang, Y.; Song, S.; Xu, C.; Hu, N.; Molenda, J.; Lu, L. Development of Solid-State Electrolytes for Sodium-Ion Battery–A Short Review. *Nano Mater. Sci.* **2019**, *1*, 91–100. [CrossRef]
37. Singh, B.; Wang, Z.; Park, S.; Gautam, G.S.; Chotard, J.-N.; Croguennec, L.; Carlier, D.; Cheetham, A.K.; Masquelier, C.; Canepa, P. A Chemical Map of NaSICON Electrode Materials for Sodium-Ion Batteries. *J. Mater. Chem. A* **2021**, *9*, 281–292. [CrossRef]
38. Zhang, L.; Liu, Y.; You, Y.; Vinu, A.; Mai, L. NASICONs-type Solid-state Electrolytes: The History, Physicochemical Properties, and Challenges. *Interdiscip. Mater.* **2022**, *2*, 91–110. [CrossRef]

39. Morimoto, H.; Awano, H.; Terashima, J.; Shindo, Y.; Nakanishi, S.; Ito, N.; Ishikawa, K.; Tobishima, S. Preparation of Lithium Ion Conducting Solid Electrolyte of NASICON-Type $Li_{1+x}Al_xTi_{2-x}(PO_4)_3$ (x = 0.3) Obtained by Using the Mechanochemical Method and Its Application as Surface Modification Materials of $LiCoO_2$ Cathode for Lithium Cell. *J. Power Sources* **2013**, *240*, 636–643. [CrossRef]
40. Dudney, N.J. Thin Film Micro-Batteries. *Electrochem. Soc. Interface* **2008**, *17*, 44–48. [CrossRef]
41. Kim, J.G.; Son, B.; Mukherjee, S.; Schuppert, N.; Bates, A.; Kwon, O.; Choi, M.J.; Chung, H.Y.; Park, S. A Review of Lithium and Non-Lithium Based Solid State Batteries. *J. Power Sources* **2015**, *282*, 299–322. [CrossRef]
42. Wei, R.; Chen, S.; Gao, T.; Liu, W. Challenges, Fabrications and Horizons of Oxide Solid Electrolytes for Solid-state Lithium Batteries. *Nano Sel.* **2021**, *2*, 2256–2274. [CrossRef]
43. Kim, A.; Woo, S.; Kang, M.; Park, H.; Kang, B. Research Progresses of Garnet-Type Solid Electrolytes for Developing All-Solid-State Li Batteries. *Front. Chem.* **2020**, *8*, 468. [CrossRef]
44. Reddy, M.V.; Julien, C.M.; Mauger, A.; Zaghib, K. Sulfide and Oxide Inorganic Solid Electrolytes for All-Solid-State Li Batteries: A Review. *Nanomaterials* **2020**, *10*, 1606. [CrossRef]
45. Murugan, R.; Thangadurai, V.; Weppner, W. Fast Lithium Ion Conduction in Garnet-Type $Li_7La_3Zr_2O_{12}$. *Angew. Chem. Int. Ed.* **2007**, *46*, 7778–7781. [CrossRef] [PubMed]
46. Li, P.; Ma, Z.; Shi, J.; Han, K.; Wan, Q.; Liu, Y.; Qu, X. Recent Advances and Perspectives of Air Stable Sulfide-Based Solid Electrolytes for All-Solid-State Lithium Batteries. *Chem. Rec.* **2022**, *22*, e202200086. [CrossRef] [PubMed]
47. Minami, K.; Mizuno, F.; Hayashi, A.; Tatsumisago, M. Lithium Ion Conductivity of the Li_2S–P_2S_5 Glass-Based Electrolytes Prepared by the Melt Quenching Method. *Solid State Ion.* **2007**, *178*, 837–841. [CrossRef]
48. Kamaya, N.; Homma, K.; Yamakawa, Y.; Hirayama, M.; Kanno, R.; Yonemura, M.; Kamiyama, T.; Kato, Y.; Hama, S.; Kawamoto, K.; et al. A Lithium Superionic Conductor. *Nat. Mater.* **2011**, *10*, 682–686. [CrossRef]
49. Kanno, R.; Murayama, M. Lithium Ionic Conductor Thio-LISICON: The Li_2S GeS_2 P_2S_5 System. *J. Electrochem. Soc.* **2001**, *148*, A742. [CrossRef]
50. Kato, Y.; Hori, S.; Saito, T.; Suzuki, K.; Hirayama, M.; Mitsui, A.; Yonemura, M.; Iba, H.; Kanno, R. High-Power All-Solid-State Batteries Using Sulfide Superionic Conductors. *Nat. Energy* **2016**, *1*, 16030. [CrossRef]
51. Aswathy, P.; Suriyakumar, S.; Kumar, S.A.; Oliyantakath Hassan, M.S.; Vijayan, V.; Shaijumon, M.M. Microwave-Assisted Synthesis of Sulfide Solid Electrolytes for All-Solid-State Sodium Batteries. *ACS Appl. Energy Mater.* **2022**, *5*, 12592–12601. [CrossRef]
52. Manthiram, A.; Yu, X.; Wang, S. Lithium Battery Chemistries Enabled by Solid-State Electrolytes. *Nat. Rev. Mater.* **2017**, *2*, 16103. [CrossRef]
53. Heo, J.W.; Banerjee, A.; Park, K.H.; Jung, Y.S.; Hong, S. New Na-Ion Solid Electrolytes $Na_{4-x}Sn_{1-x}Sb_xS_4$ ($0.02 \leq x \leq 0.33$) for All-Solid-State Na-Ion Batteries. *Adv. Energy Mater.* **2018**, *8*, 1702716. [CrossRef]
54. Bieker, G.; Küpers, V.; Kolek, M.; Winter, M. Intrinsic Differences and Realistic Perspectives of Lithium-Sulfur and Magnesium-Sulfur Batteries. *Commun. Mater.* **2021**, *2*, 37. [CrossRef]
55. Suci, W.G.; Aliwarga, H.K.; Azinuddin, Y.R.; Setyawati, R.B.; Stulasti, K.N.R.; Purwanto, A. Review of Various Sulfide Electrolyte Types for Solid-State Lithium-Ion Batteries. *Open Eng.* **2022**, *12*, 409–423. [CrossRef]
56. Su, H.; Jiang, Z.; Liu, Y.; Li, J.; Gu, C.; Wang, X.; Xia, X.; Tu, J. Recent Progress of Sulfide Electrolytes for All-Solid-State Lithium Batteries. *Energy Mater.* **2022**, *2*, 200005. [CrossRef]
57. Yu, T.; Ke, B.; Li, H.; Guo, S.; Zhou, H. Recent Advances in Sulfide Electrolytes toward High Specific Energy Solid-State Lithium Batteries. *Mater. Chem. Front.* **2021**, *5*, 4892–4911. [CrossRef]
58. Kim, S.; Oguchi, H.; Toyama, N.; Sato, T.; Takagi, S.; Otomo, T.; Arunkumar, D.; Kuwata, N.; Kawamura, J.; Orimo, S. A Complex Hydride Lithium Superionic Conductor for High-Energy-Density All-Solid-State Lithium Metal Batteries. *Nat. Commun.* **2019**, *10*, 1081. [CrossRef] [PubMed]
59. Maekawa, H.; Matsuo, M.; Takamura, H.; Ando, M.; Noda, Y.; Karahashi, T.; Orimo, S. Halide-Stabilized $LiBH_4$, a Room-Temperature Lithium Fast-Ion Conductor. *J. Am. Chem. Soc.* **2009**, *131*, 894–895. [CrossRef] [PubMed]
60. Matsuo, M.; Orimo, S. Lithium Fast-Ionic Conduction in Complex Hydrides: Review and Prospects. *Adv. Energy Mater.* **2011**, *1*, 161–172. [CrossRef]
61. Yan, Y.; Kühnel, R.; Remhof, A.; Duchêne, L.; Reyes, E.C.; Rentsch, D.; Łodziana, Z.; Battaglia, C. A Lithium Amide-Borohydride Solid-State Electrolyte with Lithium-Ion Conductivities Comparable to Liquid Electrolytes. *Adv. Energy Mater.* **2017**, *7*, 1700294. [CrossRef]
62. Tang, W.S.; Matsuo, M.; Wu, H.; Stavila, V.; Zhou, W.; Talin, A.A.; Soloninin, A.V.; Skoryunov, R.V.; Babanova, O.A.; Skripov, A.V.; et al. Liquid-Like Ionic Conduction in Solid Lithium and Sodium Monocarba-*closo*-Decaborates Near or at Room Temperature. *Adv. Energy Mater.* **2016**, *6*, 1502237, Correction in *Adv. Energy Mater.* **2016**, *6*, 1670139. [CrossRef]
63. Sadikin, Y.; Brighi, M.; Schouwink, P.; Černý, R. Superionic Conduction of Sodium and Lithium in Anion-Mixed Hydroborates $Na_3BH_4B_{12}H_{12}$ and $(Li_{0.7}Na_{0.3})_3BH_4B_{12}H_{12}$. *Adv. Energy Mater.* **2015**, *5*, 1501016. [CrossRef]
64. Cuan, J.; Zhou, Y.; Zhou, T.; Ling, S.; Rui, K.; Guo, Z.; Liu, H.; Yu, X. Borohydride-Scaffolded Li/Na/Mg Fast Ionic Conductors for Promising Solid-State Electrolytes. *Adv. Mater.* **2018**, *31*, e1803533. [CrossRef] [PubMed]
65. Tang, W.S.; Yoshida, K.; Soloninin, A.V.; Skoryunov, R.V.; Babanova, O.A.; Skripov, A.V.; Dimitrievska, M.; Stavila, V.; Orimo, S.; Udovic, T.J. Stabilizing Superionic-Conducting Structures via Mixed-Anion Solid Solutions of Monocarba-*Closo*-Borate Salts. *ACS Energy Lett.* **2016**, *1*, 659–664. [CrossRef]

66. Andersson, M.S.; Stavila, V.; Skripov, A.V.; Dimitrievska, M.; Psurek, M.T.; Leão, J.B.; Babanova, O.A.; Skoryunov, R.V.; Soloninin, A.V.; Karlsson, M.; et al. Promoting Persistent Superionic Conductivity in Sodium Monocarba-*Closo*-Dodecaborate $NaCB_{11}H_{12}$ via Confinement within Nanoporous Silica. *J. Phys. Chem. C* **2021**, *125*, 16689–16699. [CrossRef]
67. Tang, W.S.; Matsuo, M.; Wu, H.; Stavila, V.; Unemoto, A.; Orimo, S.; Udovic, T.J. Stabilizing Lithium and Sodium Fast-Ion Conduction in Solid Polyhedral-Borate Salts at Device-Relevant Temperatures. *Energy Storage Mater.* **2016**, *4*, 79–83. [CrossRef]
68. Hayashi, A.; Noi, K.; Sakuda, A.; Tatsumisago, M. Superionic Glass-Ceramic Electrolytes for Room-Temperature Rechargeable Sodium Batteries. *Nat. Commun.* **2012**, *3*, 856. [CrossRef]
69. Li, X.; Liang, J.; Yang, X.; Adair, K.R.; Wang, C.; Zhao, F.; Sun, X. Progress and Perspectives on Halide Lithium Conductors for All-Solid-State Lithium Batteries. *Energy Environ. Sci.* **2020**, *13*, 1429–1461. [CrossRef]
70. Liang, J.; Li, X.; Adair, K.R.; Sun, X. Metal Halide Superionic Conductors for All-Solid-State Batteries. *Acc. Chem. Res.* **2021**, *54*, 1023–1033. [CrossRef]
71. Yu, T.; Yang, X.; Yang, R.; Bai, X.; Xu, G.; Zhao, S.; Duan, Y.; Wu, Y.; Wang, J. Progress and Perspectives on Typical Inorganic Solid-State Electrolytes. *J. Alloys Compd.* **2021**, *885*, 161013. [CrossRef]
72. Wang, C.; Liang, J.; Luo, J.; Liu, J.; Li, X.; Zhao, F.; Li, R.; Huang, H.; Zhao, S.; Zhang, L.; et al. A Universal Wet-Chemistry Synthesis of Solid-State Halide Electrolytes for All-Solid-State Lithium-Metal Batteries. *Sci. Adv.* **2021**, *7*, eabh1896. [CrossRef] [PubMed]
73. Fan, L.; Wei, S.; Li, S.; Li, Q.; Lu, Y. Recent Progress of the Solid-State Electrolytes for High-Energy Metal-Based Batteries. *Adv. Energy Mater.* **2018**, *8*, 1702657. [CrossRef]
74. Zhou, J.; Chen, Y.; Yu, Z.; Bowden, M.; Miller, Q.R.S.; Chen, P.; Schaef, H.T.; Mueller, K.T.; Lu, D.; Xiao, J.; et al. Wet-Chemical Synthesis of $Li_7P_3S_{11}$ with Tailored Particle Size for Solid State Electrolytes. *Chem. Eng. J.* **2022**, *429*, 132334. [CrossRef]
75. Jo, Y.-S.; Hong, J.-W.; Choi, I.-H.; Sung, J.; Park, J.-H.; Park, H.; Kim, D.; Kim, B.G.; Ha, Y.-C.; Seo, J.; et al. Engineering Green and Sustainable Solvents for Scalable Wet Synthesis of Sulfide Electrolytes in High-Energy-Density All-Solid-State Batteries. *Green Chem.* **2023**, *25*, 1473–1487. [CrossRef]
76. Zhao, S.; Jiang, W.; Zhu, X.; Ling, M.; Liang, C. Understanding the Synthesis of Inorganic Solid-State Electrolytes for Li Ion Batteries: Features and Progress. *Sustain. Mater. Technol.* **2022**, *33*, e00491. [CrossRef]
77. Martinez, V.; Stolar, T.; Karadeniz, B.; Brekalo, I.; Užarević, K. Advancing Mechanochemical Synthesis by Combining Milling with Different Energy Sources. *Nat. Rev. Chem.* **2022**, *7*, 51–65. [CrossRef] [PubMed]
78. Liu, X.; Li, Y.; Zeng, L.; Li, X.; Chen, N.; Bai, S.; He, H.; Wang, Q.; Zhang, C. A Review on Mechanochemistry: Approaching Advanced Energy Materials with Greener Force. *Adv. Mater.* **2022**, *34*, 2108327. [CrossRef] [PubMed]
79. Beamish-Cook, J.; Shankland, K.; Murray, C.A.; Vaqueiro, P. Insights into the Mechanochemical Synthesis of MOF-74. *Cryst. Growth Des.* **2021**, *21*, 3047–3055. [CrossRef]
80. Do, J.-L.; Friščić, T. Mechanochemistry: A Force of Synthesis. *ACS Cent. Sci.* **2016**, *3*, 13–19. [CrossRef]
81. Ayoub, G.; Karadeniz, B.; Howarth, A.J.; Farha, O.K.; Đilović, I.; Germann, L.S.; Dinnebier, R.E.; Užarević, K.; Friščić, T. Rational Synthesis of Mixed-Metal Microporous Metal–Organic Frameworks with Controlled Composition Using Mechanochemistry. *Chem. Mater.* **2019**, *31*, 5494–5501. [CrossRef]
82. Głowniak, S.; Szczęśniak, B.; Choma, J.; Jaroniec, M. Mechanochemistry: Toward Green Synthesis of Metal–Organic Frameworks. *Mater. Today* **2021**, *46*, 109–124. [CrossRef]
83. Stolar, T.; Užarević, K. Mechanochemistry: An Efficient and Versatile Toolbox for Synthesis, Transformation, and Functionalization of Porous Metal–Organic Frameworks. *CrystEngComm* **2020**, *22*, 4511–4525. [CrossRef]
84. Užarević, K.; Wang, T.C.; Moon, S.-Y.; Fidelli, A.M.; Hupp, J.T.; Farha, O.K.; Friščić, T. Mechanochemical and Solvent-Free Assembly of Zirconium-Based Metal–Organic Frameworks. *Chem. Commun.* **2016**, *52*, 2133–2136. [CrossRef]
85. Pagola, S. Outstanding Advantages, Current Drawbacks, and Significant Recent Developments in Mechanochemistry: A Perspective View. *Crystals* **2023**, *13*, 124. [CrossRef]
86. Kim, J.W.; Shim, J.-H.; Ahn, J.-P.; Cho, Y.W.; Kim, J.-H.; Oh, K.H. Mechanochemical Synthesis and Characterization of TiB_2 and VB_2 Nanopowders. *Mater. Lett.* **2008**, *62*, 2461–2464. [CrossRef]
87. Halasz, I.; Friščić, T.; Kimber, S.A.J.; Užarević, K.; Puškarić, A.; Mottillo, C.; Julien, P.; Štrukil, V.; Honkimäki, V.; Dinnebier, R.E. Quantitative in Situ and Real-Time Monitoring of Mechanochemical Reactions. *Faraday Discuss.* **2014**, *170*, 203–221. [CrossRef] [PubMed]
88. Halasz, I.; Puškarić, A.; Kimber, S.A.J.; Beldon, P.J.; Belenguer, A.M.; Adams, F.; Honkimäki, V.; Dinnebier, R.E.; Patel, B.; Jones, W.; et al. Real-Time In Situ Powder X-ray Diffraction Monitoring of Mechanochemical Synthesis of Pharmaceutical Cocrystals. *Angew. Chem. Int. Ed.* **2013**, *52*, 11538–11541. [CrossRef] [PubMed]
89. Černý, R.; Penin, N.; Hagemann, H.; Filinchuk, Y. The First Crystallographic and Spectroscopic Characterization of a 3d-Metal Borohydride: $Mn(BH_4)_2$. *J. Phys. Chem. C* **2009**, *113*, 9003–9007, Correction in *J. Phys. Chem. C* **2009**, *113*, 14582. [CrossRef]
90. Ravnsbæk, D.; Filinchuk, Y.; Cerenius, Y.; Jakobsen, H.J.; Besenbacher, F.; Skibsted, J.; Jensen, T.R. A Series of Mixed-Metal Borohydrides. *Angew. Chem. Int. Ed.* **2009**, *48*, 6659–6663. [CrossRef] [PubMed]
91. Llamas Jansa, I.; Kalantzopoulos, G.N.; Nordholm, K.; Hauback, B.C. Destabilization of $NaBH_4$ by Transition Metal Fluorides. *Molecules* **2020**, *25*, 780. [CrossRef] [PubMed]
92. Olsen, J.E.; Sørby, M.H.; Hauback, B.C. Chloride-Substitution in Sodium Borohydride. *J. Alloys Compd.* **2011**, *509*, L228–L231. [CrossRef]

93. Doppiu, S.; Schultz, L.; Gutfleisch, O. In Situ Pressure and Temperature Monitoring during the Conversion of Mg into MgH_2 by High-Pressure Reactive Ball Milling. *J. Alloys Compd.* **2007**, *427*, 204–208. [CrossRef]
94. Fichtner, M.; Frommen, C.; Fuhr, O. Synthesis and Properties of Calcium Alanate and Two Solvent Adducts. *Inorg. Chem.* **2005**, *44*, 3479–3484. [CrossRef]
95. Brinks, H.W.; Istad-Lem, A.; Hauback, B.C. Mechanochemical Synthesis and Crystal Structure of α′-AlD3 and α-AlD3. *J. Phys. Chem. B* **2006**, *110*, 25833–25837. [CrossRef]
96. Kuziora, P.; Wyszyńska, M.; Polanski, M.; Bystrzycki, J. Why the Ball to Powder Ratio (BPR) Is Insufficient for Describing the Mechanical Ball Milling Process. *Int. J. Hydrogen Energy* **2014**, *39*, 9883–9887. [CrossRef]
97. Sadikin, Y.; Stare, K.; Schouwink, P.; Brix Ley, M.; Jensen, T.R.; Meden, A.; Černý, R. Alkali Metal—Yttrium Borohydrides: The Link between Coordination of Small and Large Rare-Earth. *J. Solid State Chem.* **2015**, *225*, 231–239. [CrossRef]
98. Černý, R.; Severa, G.; Ravnsbæk, D.B.; Filinchuk, Y.; D'Anna, V.; Hagemann, H.; Haase, D.; Jensen, C.M.; Jensen, T.R. $NaSc(BH_4)_4$: A Novel Scandium-Based Borohydride. *J. Phys. Chem. C* **2009**, *114*, 1357–1364. [CrossRef]
99. Hagemann, H.; Longhini, M.; Kaminski, J.W.; Wesolowski, T.A.; Černý, R.; Penin, N.; Sørby, M.H.; Hauback, B.C.; Severa, G.; Jensen, C.M. $LiSc(BH_4)_4$: A Novel Salt of Li+ and Discrete $Sc(BH_4)_4^-$ Complex Anions. *J. Phys. Chem. A* **2008**, *112*, 7551–7555. [CrossRef] [PubMed]
100. Solinas, I.; Lutz, H.D. Nonceramic Preparation Techniques for Ternary Halides AB_2X_4 with A = Mg, Mn, Zn; B = Li, Na; X = Cl, Br. *J. Solid State Chem.* **1995**, *117*, 34–38. [CrossRef]
101. Černý, R.; Schouwink, P.; Sadikin, Y.; Stare, K.; Smrčok, L.; Richter, B.; Jensen, T.R. Trimetallic Borohydride $Li_3MZn_5(BH_4)_{15}$ (M = Mg, Mn) Containing Two Weakly Interconnected Frameworks. *Inorg. Chem.* **2013**, *52*, 9941–9947. [CrossRef]
102. Ravnsbæk, D.B.; Sørensen, L.H.; Filinchuk, Y.; Reed, D.; Book, D.; Jakobsen, H.J.; Besenbacher, F.; Skibsted, J.; Jensen, T.R. Mixed-Anion and Mixed-Cation Borohydride $KZn(BH_4)Cl_2$: Synthesis, Structure and Thermal Decomposition. *Eur. J. Inorg. Chem.* **2010**, *2010*, 1608–1612. [CrossRef]
103. Černý, R.; Ravnsbæk, D.B.; Schouwink, P.; Filinchuk, Y.; Penin, N.; Teyssier, J.; Smrčok, L.; Jensen, T.R. Potassium Zinc Borohydrides Containing Triangular $[Zn(BH_4)_3]^-$ and Tetrahedral $[Zn(BH_4)_xCl_{4-x}]_2^-$ Anions. *J. Phys. Chem. C* **2011**, *116*, 1563–1571. [CrossRef]
104. Rude, L.H.; Zavorotynska, O.; Arnbjerg, L.M.; Ravnsbæk, D.B.; Malmkjær, R.A.; Grove, H.; Hauback, B.C.; Baricco, M.; Filinchuk, Y.; Besenbacher, F.; et al. Bromide Substitution in Lithium Borohydride, $LiBH_4$–LiBr. *Int. J. Hydrogen Energy* **2011**, *36*, 15664–15672. [CrossRef]
105. Ravnsbæk, D.B.; Ley, M.B.; Lee, Y.-S.; Hagemann, H.; D'Anna, V.; Cho, Y.W.; Filinchuk, Y.; Jensen, T.R. A Mixed-Cation Mixed-Anion Borohydride $NaY(BH_4)_2Cl_2$. *Int. J. Hydrogen Energy* **2012**, *37*, 8428–8438. [CrossRef]
106. Ley, M.B.; Boulineau, S.; Janot, R.; Filinchuk, Y.; Jensen, T.R. New Li Ion Conductors and Solid State Hydrogen Storage Materials: $LiM(BH_4)_3Cl$, M = La, Gd. *J. Phys. Chem. C* **2012**, *116*, 21267–21276. [CrossRef]
107. Matsuo, M.; Remhof, A.; Martelli, P.; Caputo, R.; Ernst, M.; Miura, Y.; Sato, T.; Oguchi, H.; Maekawa, H.; Takamura, H.; et al. Complex Hydrides with $(BH_4)^-$ and $(NH_2)^-$ Anions as New Lithium Fast-Ion Conductors. *J. Am. Chem. Soc.* **2009**, *131*, 16389–16391. [CrossRef]
108. Noritake, T.; Miwa, K.; Aoki, M.; Matsumoto, M.; Towata, S.; Li, H.-W.; Orimo, S. Synthesis and Crystal Structure Analysis of Complex Hydride $Mg(BH_4)(NH_2)$. *Int. J. Hydrogen Energy* **2013**, *38*, 6730–6735. [CrossRef]
109. Somer, M.; Acar, S.; Koz, C.; Kokal, I.; Höhn, P.; Cardoso-Gil, R.; Aydemir, U.; Akselrud, L. α- and β-$Na_2[BH_4][NH_2]$: Two Modifications of a Complex Hydride in the System $NaNH_2$–$NaBH_4$; Syntheses, Crystal Structures, Thermal Analyses, Mass and Vibrational Spectra. *J. Alloys Compd.* **2010**, *491*, 98–105. [CrossRef]
110. Tuan, L.; Nguyen, C.K.; Huan, T.D. First-Principles Prediction for the Stability of $LiK(BH_4)_2$. *Phys. Status Solidi (B)* **2014**, *251*, 1539–1544. [CrossRef]
111. Jensen, S.R.H.; Jepsen, L.H.; Skibsted, J.; Jensen, T.R. Phase Diagram for the $NaBH_4$–KBH_4 System and the Stability of a $Na_{1-x}K_xBH_4$ Solid Solution. *J. Phys. Chem. C* **2015**, *119*, 27919–27929. [CrossRef]
112. Huot, J.; Cuevas, F.; Deledda, S.; Edalati, K.; Filinchuk, Y.; Grosdidier, T.; Hauback, B.C.; Heere, M.; Jensen, T.R.; Latroche, M.; et al. Mechanochemistry of Metal Hydrides: Recent Advances. *Materials* **2019**, *12*, 2778. [CrossRef] [PubMed]
113. Huot, J.; Ravnsbæk, D.B.; Zhang, J.; Cuevas, F.; Latroche, M.; Jensen, T.R. Mechanochemical Synthesis of Hydrogen Storage Materials. *Prog. Mater. Sci.* **2013**, *58*, 30–75. [CrossRef]
114. Burazer, S.; Morelle, F.; Filinchuk, Y.; Černý, R.; Popović, J. Mixed-Metal Imidazolates Containing Alkali and Alkaline Earth Metals: Mechanochemical Synthesis and Crystal Structure of $AMgIm_3$ (A = Na or K). *Inorg. Chem.* **2019**, *58*, 6927–6933. [CrossRef] [PubMed]
115. Burazer, S.; Robeyns, K.; Guénée, L.; Mali, G.; Morelle, F.; Ban, V.; Klaser, T.; Filinchuk, Y.; Černý, R.; Popović, J. Quenchable Porous High-Temperature Polymorph of Sodium Imidazolate, NaIm. *Cryst. Growth Des.* **2021**, *21*, 770–778. [CrossRef]
116. Burazer, S.; Horák, L.; Filinchuk, Y.; Černý, R.; Popović, J. Abrupt Change from Moderate Positive to Colossal Negative Thermal Expansion Caused by Imidazolate Composite Formation. *J. Mater. Sci.* **2022**, *57*, 11563–11581. [CrossRef]
117. Fernandez-Diaz, L.; Castillo, J.; Sasieta-Barrutia, E.; Arnaiz, M.; Cabello, M.; Judez, X.; Terry, A.; Otaegui, L.; Morant-Miñana, M.C.; Villaverde, A. Mixing Methods for Solid State Electrodes: Techniques, Fundamentals, Recent Advances, and Perspectives. *Chem. Eng. J.* **2023**, *464*, 142469. [CrossRef]

118. Peng, J.; Gao, Y.; Zhang, H.; Liu, Z.; Zhang, W.; Li, L.; Qiao, Y.; Yang, W.; Wang, J.; Dou, S.; et al. Ball Milling Solid-State Synthesis of Highly Crystalline Prussian Blue Analogue $Na_{2-x}MnFe(CN)_6$ Cathodes for All-Climate Sodium-Ion Batteries. *Angew. Chem. Int. Ed.* **2022**, *61*, e202205867. [CrossRef] [PubMed]
119. Feng, D.; Xu, D.; Wang, Q.; Liu, P. Highly Stretchable Electromagnetic Interference (EMI) Shielding Segregated Polyurethane/Carbon Nanotube Composites Fabricated by Microwave Selective Sintering. *J. Mater. Chem. C* **2019**, *7*, 7938–7946. [CrossRef]
120. Sandu, G.; Ernould, B.; Rolland, J.; Cheminet, N.; Brassinne, J.; Das, P.R.; Filinchuk, Y.; Cheng, L.; Komsiyska, L.; Dubois, P.; et al. Mechanochemical Synthesis of PEDOT:PSS Hydrogels for Aqueous Formulation of Li-Ion Battery Electrodes. *ACS Appl. Mater. Interfaces* **2017**, *9*, 34865–34874. [CrossRef]
121. Kim, S.Y.; Cha, H.; Kostecki, R.; Chen, G. Composite Cathode Design for High-Energy All-Solid-State Lithium Batteries with Long Cycle Life. *ACS Energy Lett.* **2022**, *8*, 521–528. [CrossRef]
122. Zhang, J.; Yan, W.; Bai, C.G.; Luo, X.D.; Pan, F.S. Mechanochemical Synthesis of Nanocrystalline Mg-Based Hydrogen Storage Composites in Hydrogen Alloying Mills. *Mater. Sci. Forum* **2009**, *610–613*, 955–959. [CrossRef]
123. Sakuda, A. Favorable Composite Electrodes for All-Solid-State Batteries. *J. Ceram. Soc. Jpn.* **2018**, *126*, 675–683. [CrossRef]
124. Mansurov, Z.A.; Mofa, N.N.; Ketegenov, T.A.; Sadykov, B.S. *Mechanochemical Synthesis of Composite Materials*; CRC Press: Boca Raton, FL, USA, 2022.
125. Zherebtcov, I.S.; Osadchy, A.V.; Savin, V.V.; Savina, L.A.; Chaika, V.A. Synthesis of Powder Functional Composite Materials Containing G-C_3N_4, β-Si_3N_4 and Si_2N_2O Phases. *J. Phys. Conf. Ser.* **2022**, *2388*, 012013. [CrossRef]
126. Zhang, Z.; Wang, X.; Li, X.; Zhao, J.; Liu, G.; Yu, W.; Dong, X.; Wang, J. Review on Composite Solid Electrolytes for Solid-State Lithium-Ion Batteries. *Mater. Today Sustain.* **2023**, *21*, 100316. [CrossRef]
127. Gulino, V.; Longo, A.; de Kort, L.M.; Rodenburg, H.P.; Murgia, F.; Brighi, M.; Černý, R.; Sahle, C.J.; Sundermann, M.; Gretarsson, H.; et al. Anomalous Impact of Mechanochemical Treatment on the Na-ion Conductivity of Sodium *Closo*-Carbadodecaborate Probed by X-Ray Raman Scattering Spectroscopy. *Small Methods* **2023**, *8*, e2300833. [CrossRef] [PubMed]
128. Liang, H.; Wang, L.; Wang, A.; Song, Y.; Wu, Y.; Yang, Y.; He, X. Tailoring Practically Accessible Polymer/Inorganic Composite Electrolytes for All-Solid-State Lithium Metal Batteries: A Review. *Nano-Micro Lett.* **2023**, *15*, 42. [CrossRef]
129. Chien, Y.; Li, H.; Lampkin, J.; Hall, S.; Garcia-Araez, N.; Brant, W.R.; Brandell, D.; Lacey, M.J. Impact of Compression on the Electrochemical Performance of the Sulfur/Carbon Composite Electrode in Lithium-Sulfur Batteries. *Batter. Supercaps* **2022**, *5*, e202200058. [CrossRef]
130. Kubanska, A.; Castro, L.; Tortet, L.; Dollé, M.; Bouchet, R. Effect of Composite Electrode Thickness on the Electrochemical Performances of All-Solid-State Li-Ion Batteries. *J. Electroceramics* **2017**, *38*, 189–196. [CrossRef]
131. Tran, H.Y.; Greco, G.; Täubert, C.; Wohlfahrt-Mehrens, M.; Haselrieder, W.; Kwade, A. Influence of Electrode Preparation on the Electrochemical Performance of $LiNi_{0.8}Co_{0.15}Al_{0.05}O_2$ Composite Electrodes for Lithium-Ion Batteries. *J. Power Sources* **2012**, *210*, 276–285. [CrossRef]
132. Gonzalez, G.; Gonzalez, R.; Zuniga, L.; Chipara, M.; Alcoutlabi, M. The Effect of Carbon Coatings on the Electrochemical Performance of Composite Electrodes. *ECS Trans.* **2020**, *97*, 93–104. [CrossRef]
133. Zhang, X.; Weng, J.; Ye, C.; Liu, M.; Wang, C.; Wu, S.; Tong, Q.; Zhu, M.; Gao, F. Strategies for Controlling or Releasing the Influence Due to the Volume Expansion of Silicon inside Si–C Composite Anode for High-Performance Lithium-Ion Batteries. *Materials* **2022**, *15*, 4264. [CrossRef] [PubMed]
134. Yamamoto, M.; Takahashi, M.; Terauchi, Y.; Kobayashi, Y.; Ikeda, S.; Sakuda, A. Fabrication of Composite Positive Electrode Sheet with High Active Material Content and Effect of Fabrication Pressure for All-Solid-State Battery. *J. Ceram. Soc. Jpn.* **2017**, *125*, 391–395. [CrossRef]
135. Burazer, S.; Sopčić, S.; Mandić, Z. Anodic Deposition of Lead Dioxide at Nafion® Covered Gold Electrode. *J. Solid State Electrochem.* **2016**, *20*, 3053–3059. [CrossRef]
136. Nguyen, Q.H.; Kim, H.; Kim, I.T.; Choi, W.; Hur, J. Few-Layer $NbSe_2$@graphene Heterostructures as Anodes in Lithium-Ion Half- and Full-Cell Batteries. *Chem. Eng. J.* **2020**, *382*, 122981. [CrossRef]
137. Université de Genève (UNIGE). Un Nouvel Électrolyte pour des Piles Plus sûres/A New Electrolyte for Greener and Safer Batteries. Available online: https://www.youtube.com/watch?v=xFbNXayYMSE (accessed on 16 November 2023).
138. Wang, L.; Li, J.; Lu, G.; Li, W.; Tao, Q.; Shi, C.; Jin, H.; Chen, G.; Wang, S. Fundamentals of Electrolytes for Solid-State Batteries: Challenges and Perspectives. *Front. Mater.* **2020**, *7*, 111. [CrossRef]
139. Yang, H.-L.; Zhang, B.-W.; Konstantinov, K.; Wang, Y.-X.; Liu, H.-K.; Dou, S.-X. Progress and Challenges for All-Solid-State Sodium Batteries. *Adv. Energy Sustain. Res.* **2021**, *2*, 2000057. [CrossRef]
140. Chen, W.; Lei, T.; Wu, C.; Deng, M.; Gong, C.; Hu, K.; Ma, Y.; Dai, L.; Lv, W.; He, W.; et al. Designing Safe Electrolyte Systems for a High-Stability Lithium–Sulfur Battery. *Adv. Energy Mater.* **2018**, *8*, 1702348. [CrossRef]
141. Chen, Y.; Zhuo, S.; Li, Z.; Wang, C. Redox Polymers for Rechargeable Metal-Ion Batteries. *EnergyChem* **2020**, *2*, 100030. [CrossRef]
142. Wang, S.; Xu, H.; Li, W.; Dolocan, A.; Manthiram, A. Interfacial Chemistry in Solid-State Batteries: Formation of Interphase and Its Consequences. *J. Am. Chem. Soc.* **2017**, *140*, 250–257. [CrossRef] [PubMed]
143. Miura, A.; Rosero-Navarro, N.C.; Sakuda, A.; Tadanaga, K.; Phuc, N.H.H.; Matsuda, A.; Machida, N.; Hayashi, A.; Tatsumisago, M. Liquid-Phase Syntheses of Sulfide Electrolytes for All-Solid-State Lithium Battery. *Nat. Rev. Chem.* **2019**, *3*, 189–198. [CrossRef]
144. Han, X.; Gong, Y.; Fu, K.; He, X.; Hitz, G.T.; Dai, J.; Pearse, A.; Liu, B.; Wang, H.; Rubloff, G.; et al. Negating Interfacial Impedance in Garnet-Based Solid-State Li Metal Batteries. *Nat. Mater.* **2016**, *16*, 572–579. [CrossRef] [PubMed]

145. Famprikis, T.; Canepa, P.; Dawson, J.A.; Islam, M.S.; Masquelier, C. Fundamentals of Inorganic Solid-State Electrolytes for Batteries. *Nat. Mater.* **2019**, *18*, 1278–1291. [CrossRef] [PubMed]
146. Kerman, K.; Luntz, A.; Viswanathan, V.; Chiang, Y.-M.; Chen, Z. Review—Practical Challenges Hindering the Development of Solid State Li Ion Batteries. *J. Electrochem. Soc.* **2017**, *164*, A1731–A1744. [CrossRef]
147. Strauss, F.; Bartsch, T.; de Biasi, L.; Kim, A.-Y.; Janek, J.; Hartmann, P.; Brezesinski, T. Impact of Cathode Material Particle Size on the Capacity of Bulk-Type All-Solid-State Batteries. *ACS Energy Lett.* **2018**, *3*, 992–996. [CrossRef]
148. Zhao, Q.; Stalin, S.; Zhao, C.-Z.; Archer, L.A. Designing Solid-State Electrolytes for Safe, Energy-Dense Batteries. *Nat. Rev. Mater.* **2020**, *5*, 229–252. [CrossRef]
149. Bachman, J.C.; Muy, S.; Grimaud, A.; Chang, H.-H.; Pour, N.; Lux, S.F.; Paschos, O.; Maglia, F.; Lupart, S.; Lamp, P.; et al. Inorganic Solid-State Electrolytes for Lithium Batteries: Mechanisms and Properties Governing Ion Conduction. *Chem. Rev.* **2015**, *116*, 140–162. [CrossRef]
150. Boukamp, B.A.; Huggins, R.A. Lithium-Ion Conductivity in Lithium Nitride. *Phys. Lett. A* **1976**, *58*, 231–233. [CrossRef]
151. Zhao, Y.; Daemen, L.L. Superionic Conductivity in Lithium-Rich Anti-Perovskites. *J. Am. Chem. Soc.* **2012**, *134*, 15042–15047. [CrossRef]
152. Zheng, F.; Kotobuki, M.; Song, S.; Lai, M.O.; Lu, L. Review on Solid Electrolytes for All-Solid-State Lithium-Ion Batteries. *J. Power Sources* **2018**, *389*, 198–213. [CrossRef]
153. Hong, H.Y.-P. Crystal Structure and Ionic Conductivity of $Li_{14}Zn(GeO_4)_4$ and Other New Li^+ Superionic Conductors. *Mater. Res. Bull.* **1978**, *13*, 117–124. [CrossRef]
154. Bates, J.B.; Dudney, N.J.; Gruzalski, G.R.; Zuhr, R.A.; Choudhury, A.; Luck, C.F.; Robertson, J.D. Fabrication and Characterization of Amorphous Lithium Electrolyte Thin Films and Rechargeable Thin-Film Batteries. *J. Power Sources* **1993**, *43*, 103–110. [CrossRef]
155. He, L.; Lin, H.; Li, H.-F.; Filinchuk, Y.; Zhang, J.; Liu, Y.; Yang, M.; Hou, Y.; Deng, Y.; Li, H.-W.; et al. $Na_3NH_2B_{12}H_{12}$ as High Performance Solid Electrolyte for All-Solid-State Na-Ion Batteries. *J. Power Sources* **2018**, *396*, 574–579. [CrossRef]
156. Ohno, S.; Zeier, W.G. Sodium Is the New Lithium. *Nat. Energy* **2022**, *7*, 686–687. [CrossRef]
157. Pross-Brakhage, J.; Fitz, O.; Bischoff, C.; Biro, D.; Birke, K.P. Post-Lithium Batteries with Zinc for the Energy Transition. *Batteries* **2023**, *9*, 367. [CrossRef]
158. Zhao, C.; Liu, L.; Qi, X.; Lu, Y.; Wu, F.; Zhao, J.; Yu, Y.; Hu, Y.; Chen, L. Solid-State Sodium Batteries. *Adv. Energy Mater.* **2018**, *8*, 1703012. [CrossRef]
159. Zhang, Z.; Shao, Y.; Lotsch, B.; Hu, Y.-S.; Li, H.; Janek, J.; Nazar, L.F.; Nan, C.-W.; Maier, J.; Armand, M.; et al. New Horizons for Inorganic Solid State Ion Conductors. *Energy Environ. Sci.* **2018**, *11*, 1945–1976. [CrossRef]
160. Chi, X.; Zhang, Y.; Hao, F.; Kmiec, S.; Dong, H.; Xu, R.; Zhao, K.; Ai, Q.; Terlier, T.; Wang, L.; et al. An Electrochemically Stable Homogeneous Glassy Electrolyte Formed at Room Temperature for All-Solid-State Sodium Batteries. *Nat. Commun.* **2022**, *13*, 2854. [CrossRef] [PubMed]
161. Jin, Y.; Le, P.M.L.; Gao, P.; Xu, Y.; Xiao, B.; Engelhard, M.H.; Cao, X.; Vo, T.D.; Hu, J.; Zhong, L.; et al. Low-Solvation Electrolytes for High-Voltage Sodium-Ion Batteries. *Nat. Energy* **2022**, *7*, 718–725. [CrossRef]
162. Hayashi, A.; Masuzawa, N.; Yubuchi, S.; Tsuji, F.; Hotehama, C.; Sakuda, A.; Tatsumisago, M. A Sodium-Ion Sulfide Solid Electrolyte with Unprecedented Conductivity at Room Temperature. *Nat. Commun.* **2019**, *10*, 5266. [CrossRef]
163. Shen, X.; Zhou, Q.; Han, M.; Qi, X.; Li, B.; Zhang, Q.; Zhao, J.; Yang, C.; Liu, H.; Hu, Y.-S. Rapid Mechanochemical Synthesis of Polyanionic Cathode with Improved Electrochemical Performance for Na-Ion Batteries. *Nat. Commun.* **2021**, *12*, 2848. [CrossRef] [PubMed]
164. Ledwoch, D.; Robinson, J.B.; Gastol, D.; Smith, K.; Shearing, P.R.; Brett, D.J.L.; Kendrick, E. Hard Carbon Composite Electrodes for Sodium-Ion Batteries with Nano-Zeolite and Carbon Black Additives. *Batter. Supercaps* **2020**, *4*, 163–172. [CrossRef]
165. Hou, W.; Guo, X.; Shen, X.; Amine, K.; Yu, H.; Lu, J. Solid Electrolytes and Interfaces in All-Solid-State Sodium Batteries: Progress and Perspective. *Nano Energy* **2018**, *52*, 279–291. [CrossRef]
166. Goodenough, J.B.; Hong, H.Y.-P.; Kafalas, J.A. Fast Na+-Ion Transport in Skeleton Structures. *Mater. Res. Bull.* **1976**, *11*, 203–220. [CrossRef]
167. Hao, F.; Chi, X.; Liang, Y.; Zhang, Y.; Xu, R.; Guo, H.; Terlier, T.; Dong, H.; Zhao, K.; Lou, J.; et al. Taming Active Material-Solid Electrolyte Interfaces with Organic Cathode for All-Solid-State Batteries. *Joule* **2019**, *3*, 1349–1359. [CrossRef]
168. Wu, E.A.; Banerjee, S.; Tang, H.; Richardson, P.M.; Doux, J.-M.; Qi, J.; Zhu, Z.; Grenier, A.; Li, Y.; Zhao, E.; et al. A Stable Cathode-Solid Electrolyte Composite for High-Voltage, Long-Cycle-Life Solid-State Sodium-Ion Batteries. *Nat. Commun.* **2021**, *12*, 1256. [CrossRef]
169. Matios, E.; Wang, H.; Wang, C.; Hu, X.; Lu, X.; Luo, J.; Li, W. Graphene Regulated Ceramic Electrolyte for Solid-State Sodium Metal Battery with Superior Electrochemical Stability. *ACS Appl. Mater. Interfaces* **2019**, *11*, 5064–5072. [CrossRef]
170. Ruan, Y.; Guo, F.; Liu, J.; Song, S.; Jiang, N.; Cheng, B. Optimization of $Na_3Zr_2Si_2PO_{12}$ Ceramic Electrolyte and Interface for High Performance Solid-State Sodium Battery. *Ceram. Int.* **2019**, *45*, 1770–1776. [CrossRef]
171. Karabelli, D.; Birke, K.P.; Weeber, M. A Performance and Cost Overview of Selected Solid-State Electrolytes: Race between Polymer Electrolytes and Inorganic Sulfide Electrolytes. *Batteries* **2021**, *7*, 18. [CrossRef]
172. Duchêne, L.; Remhof, A.; Hagemann, H.; Battaglia, C. Status and Prospects of Hydroborate Electrolytes for All-Solid-State Batteries. *Energy Storage Mater.* **2020**, *25*, 782–794. [CrossRef]
173. Lou, S.; Zhang, F.; Fu, C.; Chen, M.; Ma, Y.; Yin, G.; Wang, J. Interface Issues and Challenges in All-Solid-State Batteries: Lithium, Sodium, and Beyond. *Adv. Mater.* **2020**, *33*, 2000721. [CrossRef]

174. Matsuo, M.; Nakamori, Y.; Orimo, S.; Maekawa, H.; Takamura, H. Lithium Superionic Conduction in Lithium Borohydride Accompanied by Structural Transition. *Appl. Phys. Lett.* **2007**, *91*, 224103. [CrossRef]
175. Yoshida, K.; Unemoto, A.; Oguchi, H.; Orimo, S. Complex Hydride as a Novel Solid Electrolyte and Its Application to an All-Solid-State Battery. *Mater. Jpn.* **2017**, *56*, 448–452. [CrossRef]
176. Paskevicius, M.; Pitt, M.P.; Brown, D.H.; Sheppard, D.A.; Chumphongphan, S.; Buckley, C.E. First-Order Phase Transition in the $Li_2B_{12}H_{12}$ System. *Phys. Chem. Chem. Phys.* **2013**, *15*, 15825. [CrossRef]
177. Udovic, T.J.; Matsuo, M.; Tang, W.S.; Wu, H.; Stavila, V.; Soloninin, A.V.; Skoryunov, R.V.; Babanova, O.A.; Skripov, A.V.; Rush, J.J.; et al. Exceptional Superionic Conductivity in Disordered Sodium Decahydro-*closo*-decaborate. *Adv. Mater.* **2014**, *26*, 7622–7626. [CrossRef]
178. Udovic, T.J.; Matsuo, M.; Unemoto, A.; Verdal, N.; Stavila, V.; Skripov, A.V.; Rush, J.J.; Takamura, H.; Orimo, S. Sodium Superionic Conduction in $Na_2B_{12}H_{12}$. *Chem. Commun.* **2014**, *50*, 3750–3752. [CrossRef]
179. He, L.; Li, H.-W.; Nakajima, H.; Tumanov, N.; Filinchuk, Y.; Hwang, S.-J.; Sharma, M.; Hagemann, H.; Akiba, E. Synthesis of a Bimetallic Dodecaborate $LiNaB_{12}H_{12}$ with Outstanding Superionic Conductivity. *Chem. Mater.* **2015**, *27*, 5483–5486. [CrossRef]
180. Tang, W.S.; Udovic, T.J.; Stavila, V. Altering the Structural Properties of $A_2B_{12}H_{12}$ Compounds via Cation and Anion Modifications. *J. Alloys Compd.* **2015**, *645*, S200–S204. [CrossRef]
181. Tang, W.S.; Unemoto, A.; Zhou, W.; Stavila, V.; Matsuo, M.; Wu, H.; Orimo, S.; Udovic, T.J. Unparalleled Lithium and Sodium Superionic Conduction in Solid Electrolytes with Large Monovalent Cage-like Anions. *Energy Environ. Sci.* **2015**, *8*, 3637–3645. [CrossRef]
182. de Kort, L.M.; Gulino, V.; de Jongh, P.E.; Ngene, P. Ionic Conductivity in Complex Metal Hydride-Based Nanocomposite Materials: The Impact of Nanostructuring and Nanocomposite Formation. *J. Alloys Compd.* **2022**, *901*, 163474. [CrossRef]
183. Hirose, T.; Mishina, T.; Matsui, N.; Suzuki, K.; Saito, T.; Kamiyama, T.; Hirayama, M.; Kanno, R. Fast Hydride-Ion Conduction in Perovskite Hydrides $AELiH_3$. *ACS Appl. Energy Mater.* **2022**, *5*, 2968–2974. [CrossRef]
184. Yoshida, K.; Sato, T.; Unemoto, A.; Matsuo, M.; Ikeshoji, T.; Udovic, T.J.; Orimo, S. Fast Sodium Ionic Conduction in $Na_2B_{10}H_{10}$-$Na_2B_{12}H_{12}$ Pseudo-Binary Complex Hydride and Application to a Bulk-Type All-Solid-State Battery. *Appl. Phys. Lett.* **2017**, *110*, 103901. [CrossRef]
185. Pang, Y.; Liu, Y.; Yang, J.; Zheng, S.; Wang, C. Hydrides for Solid-State Batteries: A Review. *Mater. Today Nano* **2022**, *18*, 100194. [CrossRef]
186. Zhan, Y.; Zhang, W.; Lei, B.; Liu, H.; Li, W. Recent Development of Mg Ion Solid Electrolyte. *Front. Chem.* **2020**, *8*, 125. [CrossRef]
187. Payandeh, S.; Remhof, A.; Battaglia, C. CHAPTER 3. Solid-State Magnesium-Ion Conductors. In *Magnesium Batteries Series*; Fichtner, M., Ed.; Royal Society of Chemistry Books: London, UK, 2019; pp. 60–78. [CrossRef]
188. Mohtadi, R.; Tutusaus, O.; Arthur, T.S.; Zhao-Karger, Z.; Fichtner, M. The Metamorphosis of Rechargeable Magnesium Batteries. *Joule* **2021**, *5*, 581–617. [CrossRef]
189. Gregory, T.D.; Hoffman, R.J.; Winterton, R.C. Nonaqueous Electrochemistry of Magnesium: Applications to Energy Storage. *J. Electrochem. Soc.* **1990**, *137*, 775–780. [CrossRef]
190. Aurbach, D.; Cohen, Y.; Moshkovich, M. The Study of Reversible Magnesium Deposition by In Situ Scanning Tunneling Microscopy. *Electrochem. Solid-State Lett.* **2001**, *4*, A113. [CrossRef]
191. Davidson, R.; Verma, A.; Santos, D.; Hao, F.; Fincher, C.; Xiang, S.; Van Buskirk, J.; Xie, K.; Pharr, M.; Mukherjee, P.P.; et al. Formation of Magnesium Dendrites during Electrodeposition. *ACS Energy Lett.* **2018**, *4*, 375–376. [CrossRef]
192. Jäckle, M.; Groß, A. Microscopic Properties of Lithium, Sodium, and Magnesium Battery Anode Materials Related to Possible Dendrite Growth. *J. Chem. Phys.* **2014**, *141*, 174710. [CrossRef]
193. Mohtadi, R.; Matsui, M.; Arthur, T.S.; Hwang, S. Magnesium Borohydride: From Hydrogen Storage to Magnesium Battery. *Angew. Chem. Int. Ed.* **2012**, *51*, 9780–9783. [CrossRef]
194. Zhao-Karger, Z.; Gil Bardaji, M.E.; Fuhr, O.; Fichtner, M. A New Class of Non-Corrosive, Highly Efficient Electrolytes for Rechargeable Magnesium Batteries. *J. Mater. Chem. A* **2017**, *5*, 10815–10820. [CrossRef]
195. Bockris, J.O.; Reddy, A.K.N. *Modern Electrochemistry 1*; Kluwer Academic Publishers: New York, NY, USA; Boston, MS, USA; Dordrecht, The Netherlands; London, UK; Moscow, Russia, 1998. [CrossRef]
196. Takada, K. Progress and Prospective of Solid-State Lithium Batteries. *Acta Mater.* **2013**, *61*, 759–770. [CrossRef]
197. Barbosa, J.C.; Gonçalves, R.; Costa, C.M.; Lanceros-Méndez, S. Toward Sustainable Solid Polymer Electrolytes for Lithium-Ion Batteries. *ACS Omega* **2022**, *7*, 14457–14464. [CrossRef]
198. Zhu, X.; Wang, K.; Xu, Y.; Zhang, G.; Li, S.; Li, C.; Zhang, X.; Sun, X.; Ge, X.; Ma, Y. Strategies to Boost Ionic Conductivity and Interface Compatibility of Inorganic—Organic Solid Composite Electrolytes. *Energy Storage Mater.* **2021**, *36*, 291–308. [CrossRef]
199. Park, H.; Le Mong, A.; Kim, D. Single and Multilayer Composite Electrolytes for Enhanced Li-Ion Conductivity with Restricted Polysulfide Diffusion for Lithium–Sulfur Battery. *Mater. Today Energy* **2023**, *33*, 101274. [CrossRef]
200. Hiraoka, K.; Kato, M.; Kobayashi, T.; Seki, S. Polyether/$Na_3Zr_2Si_2PO_{12}$ Composite Solid Electrolytes for All-Solid-State Sodium Batteries. *J. Phys. Chem. C* **2020**, *124*, 21948–21956. [CrossRef]
201. Niu, W.; Chen, L.; Liu, Y.; Fan, L.-Z. All-Solid-State Sodium Batteries Enabled by Flexible Composite Electrolytes and Plastic-Crystal Interphase. *Chem. Eng. J.* **2020**, *384*, 123233. [CrossRef]
202. Lim, H.-S.; Liu, L.; Lee, H.-J.; Cha, J.-M.; Yoon, D.; Ryu, B.-K. The Study on the Interface Characteristics of Solid-State Electrolyte. *J. Korean Ceram. Soc.* **2021**, *58*, 373–377. [CrossRef]

203. Oh, J.A.S.; He, L.; Plewa, A.; Morita, M.; Zhao, Y.; Sakamoto, T.; Song, X.; Zhai, W.; Zeng, K.; Lu, L. Composite NASICON ($Na_3Zr_2Si_2PO_{12}$) Solid-State Electrolyte with Enhanced Na^+ Ionic Conductivity: Effect of Liquid Phase Sintering. *ACS Appl. Mater. Interfaces* **2019**, *11*, 40125–40133. [CrossRef]
204. He, X. Hypes and Hopes of Solid-State Batteries. Available online: https://www.idtechex.com/en/research-article/hypes-and-hopes-of-solid-state-batteries/28621 (accessed on 16 November 2023).
205. Ma, Y.; Wan, J.; Xu, X.; Sendek, A.D.; Holmes, S.E.; Ransom, B.; Jiang, Z.; Zhang, P.; Xiao, X.; Zhang, W.; et al. Experimental Discovery of a Fast and Stable Lithium Thioborate Solid Electrolyte, $Li_{6+2x}[B_{10}S_{18}]S_x$ ($x \approx 1$). *ACS Energy Lett.* **2023**, *8*, 2762–2771. [CrossRef]
206. Hofer, M.; Grube, M.; Burmeister, C.F.; Michalowski, P.; Zellmer, S.; Kwade, A. Effective Mechanochemical Synthesis of Sulfide Solid Electrolyte Li_3PS_4 in a High Energy Ball Mill by Process Investigation. *Adv. Powder Technol.* **2023**, *34*, 104004. [CrossRef]
207. Banik, A.; Famprikis, T.; Ghidiu, M.; Ohno, S.; Kraft, M.A.; Zeier, W.G. On the Underestimated Influence of Synthetic Conditions in Solid Ionic Conductors. *Chem. Sci.* **2021**, *12*, 6238–6263. [CrossRef]
208. Liu, X.; Kang, W.; Li, X.; Zeng, L.; Li, Y.; Wang, Q.; Zhang, C. Solid-State Mechanochemistry Advancing Two Dimensional Materials for Lithium-Ion Storage Applications: A Mini Review. *Nano Mater. Sci.* **2023**, *5*, 210–227. [CrossRef]
209. Yu, C.; Li, Y.; Adair, K.R.; Li, W.; Goubitz, K.; Zhao, Y.; Willans, M.J.; Thijs, M.A.; Wang, C.; Zhao, F.; et al. Tuning Ionic Conductivity and Electrode Compatibility of Li_3YBr_6 for High-Performance All Solid-State Li Batteries. *Nano Energy* **2020**, *77*, 105097. [CrossRef]
210. Schlem, R.; Muy, S.; Prinz, N.; Banik, A.; Shao-Horn, Y.; Zobel, M.; Zeier, W.G. Mechanochemical Synthesis: A Tool to Tune Cation Site Disorder and Ionic Transport Properties of Li_3MCl_6 (M = Y, Er) Superionic Conductors. *Adv. Energy Mater.* **2019**, *10*, 1903719. [CrossRef]
211. Boulineau, S.; Courty, M.; Tarascon, J.-M.; Viallet, V. Mechanochemical Synthesis of Li-Argyrodite Li_6PS_5X (X = Cl, Br, I) as Sulfur-Based Solid Electrolytes for All Solid State Batteries Application. *Solid State Ion.* **2012**, *221*, 1–5. [CrossRef]
212. Asano, T.; Sakai, A.; Ouchi, S.; Sakaida, M.; Miyazaki, A.; Hasegawa, S. Solid Halide Electrolytes with High Lithium-Ion Conductivity for Application in 4 V Class Bulk-Type All-Solid-State Batteries. *Adv. Mater.* **2018**, *30*, 1803075. [CrossRef]
213. Ohno, S.; Koerver, R.; Dewald, G.; Rosenbach, C.; Titscher, P.; Steckermeier, D.; Kwade, A.; Janek, J.; Zeier, W.G. Observation of Chemomechanical Failure and the Influence of Cutoff Potentials in All-Solid-State Li–S Batteries. *Chem. Mater.* **2019**, *31*, 2930–2940. [CrossRef]
214. Ning, L.J.; Wu, Y.P.; Fang, S.B.; Rahm, E.; Holze, R. Materials Prepared for Lithium Ion Batteries by Mechanochemical Methods. *J. Power Sources* **2004**, *133*, 229–242. [CrossRef]
215. Kwak, H.; Han, D.; Lyoo, J.; Park, J.; Jung, S.H.; Han, Y.; Kwon, G.; Kim, H.; Hong, S.; Nam, K.; et al. New Cost-Effective Halide Solid Electrolytes for All-Solid-State Batteries: Mechanochemically Prepared Fe^{3+}-Substituted Li_2ZrCl_6. *Adv. Energy Mater.* **2021**, *11*, 2003190. [CrossRef]
216. Rao, R.P.; Zhang, X.; Phuah, K.C.; Adams, S. Mechanochemical Synthesis of Fast Sodium Ion Conductor $Na_{11}Sn_2PSe_{12}$ enables First Sodium–Selenium All-Solid-State Battery. *J. Mater. Chem. A* **2019**, *7*, 20790–20798. [CrossRef]
217. Roos, A.; Schoonman, J. Electronic Conductivity in $La_{1-x}Ba_xF_{3-x}$ Crystals. *Solid State Ion.* **1984**, *13*, 205–211. [CrossRef]
218. Gschwind, F.; Rodriguez-Garcia, G.; Sandbeck, D.J.S.; Gross, A.; Weil, M.; Fichtner, M.; Hörmann, N. Fluoride Ion Batteries: Theoretical Performance, Safety, Toxicity, and a Combinatorial Screening of New Electrodes. *J. Fluor. Chem.* **2016**, *182*, 76–90. [CrossRef]
219. Ruprecht, B.; Wilkening, M.; Feldhoff, A.; Steuernagel, S.; Heitjans, P. High Anion Conductivity in a Ternary Non-Equilibrium Phase of BaF_2 and CaF_2 with Mixed Cations. *Phys. Chem. Chem. Phys.* **2009**, *11*, 3071. [CrossRef]
220. Molaiyan, P.; Witter, R. Mechanochemical Synthesis of Solid-State Electrolyte $Sm_{1-x}Ca_xF_{3-x}$ for Batteries and Other Electrochemical Devices. *Mater. Lett.* **2019**, *244*, 22–26. [CrossRef]
221. Yamanaka, T.; Hayashi, A.; Yamauchi, A.; Tatsumisago, M. Preparation of Magnesium Ion Conducting $MgS–P_2S_5–MgI_2$ Glasses by a Mechanochemical Technique. *Solid State Ion.* **2014**, *262*, 601–603. [CrossRef]
222. Song, S.; Sheptyakov, D.; Korsunsky, A.M.; Duong, H.M.; Lu, L. High Li Ion Conductivity in a Garnet-Type Solid Electrolyte via Unusual Site Occupation of the Doping Ca Ions. *Mater. Des.* **2016**, *93*, 232–237. [CrossRef]
223. Ghidiu, M.; Ruhl, J.; Culver, S.P.; Zeier, W.G. Solution-Based Synthesis of Lithium Thiophosphate Superionic Conductors for Solid-State Batteries: A Chemistry Perspective. *J. Mater. Chem. A* **2019**, *7*, 17735–17753. [CrossRef]
224. Yoshida, K.; Suzuki, S.; Kawaji, J.; Unemoto, A.; Orimo, S. Complex Hydride for Composite Negative Electrode—Applicable to Bulk-Type All-Solid-State Li-Ion Battery with Wide Temperature Operation. *Solid State Ion.* **2016**, *285*, 96–100. [CrossRef]
225. Unemoto, A.; Matsuo, M.; Orimo, S. Complex Hydrides for Electrochemical Energy Storage. *Adv. Funct. Mater.* **2014**, *24*, 2267–2279. [CrossRef]
226. Duchêne, L.; Kühnel, R.-S.; Stilp, E.; Cuervo Reyes, E.; Remhof, A.; Hagemann, H.; Battaglia, C. A Stable 3 V All-Solid-State Sodium–Ion Battery Based on a *Closo*-Borate Electrolyte. *Energy Environ. Sci.* **2017**, *10*, 2609–2615. [CrossRef]
227. Sau, K.; Ikeshoji, T.; Kim, S.; Takagi, S.; Orimo, S. Comparative Molecular Dynamics Study of the Roles of Anion–Cation and Cation–Cation Correlation in Cation Diffusion in $Li_2B_{12}H_{12}$ and $LiCB_{11}H_{12}$. *Chem. Mater.* **2021**, *33*, 2357–2369. [CrossRef]
228. Murgia, F.; Brighi, M.; Černý, R. Room-Temperature-Operating Na Solid-State Battery with Complex Hydride as Electrolyte. *Electrochem. Commun.* **2019**, *106*, 106534. [CrossRef]
229. Brighi, M.; Murgia, F.; Černý, R. *Closo*-Hydroborate Sodium Salts as an Emerging Class of Room-Temperature Solid Electrolytes. *Cell Rep. Phys. Sci.* **2020**, *1*, 100217. [CrossRef]

230. Li, H.-W.; Yan, Y.; Orimo, S.; Züttel, A.; Jensen, C.M. Recent Progress in Metal Borohydrides for Hydrogen Storage. *Energies* **2011**, *4*, 185–214. [CrossRef]
231. Jena, P. Superhalogens: A Bridge between Complex Metal Hydrides and Li Ion Batteries. *J. Phys. Chem. Lett.* **2015**, *6*, 1119–1125. [CrossRef]
232. Brighi, M.; Murgia, F.; Łodziana, Z.; Schouwink, P.; Wołczyk, A.; Cerny, R. A Mixed Anion Hydroborate/Carba-Hydroborate as a Room Temperature Na-Ion Solid Electrolyte. *J. Power Sources* **2018**, *404*, 7–12. [CrossRef]
233. Orimo, S.-I.; Nakamori, Y.; Ohba, N.; Miwa, K.; Aoki, M.; Towata, S.; Züttel, A. Experimental Studies on Intermediate Compound of $LiBH_4$. *Appl. Phys. Lett.* **2006**, *89*, 021920. [CrossRef]
234. Li, H.-W.; Kikuchi, K.; Nakamori, Y.; Ohba, N.; Miwa, K.; Towata, S.; Orimo, S. Dehydriding and Rehydriding Processes of Well-Crystallized $Mg(BH_4)_2$ Accompanying with Formation of Intermediate Compounds. *Acta Mater.* **2008**, *56*, 1342–1347. [CrossRef]
235. Hwang, S.-J.; Bowman, R.C.; Reiter, J.W.; Rijssenbeek; Soloveichik, G.L.; Zhao, J.-C.; Kabbour, H.; Ahn, C.C. NMR Confirmation for Formation of $[B_{12}H_{12}]^{2-}$ Complexes during Hydrogen Desorption from Metal Borohydrides. *J. Phys. Chem. C* **2008**, *112*, 3164–3169. [CrossRef]
236. Friedrichs, O.; Remhof, A.; Hwang, S.-J.; Züttel, A. Role of $Li_2B_{12}H_{12}$ for the Formation and Decomposition of $LiBH_4$. *Chem. Mater.* **2010**, *22*, 3265–3268. [CrossRef]
237. Ozolins, V.; Majzoub, E.H.; Wolverton, C. First-Principles Prediction of Thermodynamically Reversible Hydrogen Storage Reactions in the Li-Mg-Ca-B-H System. *J. Am. Chem. Soc.* **2008**, *131*, 230–237. [CrossRef] [PubMed]
238. Züttel, A.; Wenger, P.; Rentsch, S.; Sudan, P.; Mauron, P.; Emmenegger, C. $LiBH_4$ a New Hydrogen Storage Material. *J. Power Sources* **2003**, *118*, 1–7. [CrossRef]
239. Filinchuk, Y.; Richter, B.; Jensen, T.R.; Dmitriev, V.; Chernyshov, D.; Hagemann, H. Porous and Dense Magnesium Borohydride Frameworks: Synthesis, Stability, and Reversible Absorption of Guest Species. *Angew. Chem. Int. Ed.* **2011**, *50*, 11162–11166. [CrossRef]
240. Schouwink, P.; Ley, M.B.; Tissot, A.; Hagemann, H.; Jensen, T.R.; Smrčok, Ľ.; Černý, R. Structure and Properties of Complex Hydride Perovskite Materials. *Nat. Commun.* **2014**, *5*, 5706. [CrossRef] [PubMed]
241. Pitt, M.P.; Paskevicius, M.; Brown, D.H.; Sheppard, D.A.; Buckley, C.E. Thermal Stability of $Li_2B_{12}H_{12}$ and Its Role in the Decomposition of $LiBH_4$. *J. Am. Chem. Soc.* **2013**, *135*, 6930–6941. [CrossRef] [PubMed]
242. Hueso, K.B.; Armand, M.; Rojo, T. High Temperature Sodium Batteries: Status, Challenges and Future Trends. *Energy Environ. Sci.* **2013**, *6*, 734. [CrossRef]
243. Jørgensen, M.; Jensen, S.R.H.; Humphries, T.D.; Rowles, M.R.; Sofianos, M.V.; Buckley, C.E.; Jensen, T.R.; Paskevicius, M. Hydroxylated *Closo*-Dodecaborates $M_2B_{12}(OH)_{12}$ (M = Li, Na, K, and Cs); Structural Analysis, Thermal Properties, and Solid-State Ionic Conductivity. *J. Phys. Chem. C* **2020**, *124*, 11340–11349. [CrossRef]
244. Li, H.-W.; Orimo, S.; Nakamori, Y.; Miwa, K.; Ohba, N.; Towata, S.; Züttel, A. Materials Designing of Metal Borohydrides: Viewpoints from Thermodynamical Stabilities. *J. Alloys Compd.* **2007**, *446–447*, 315–318. [CrossRef]
245. Nickels, E.A.; Jones, M.O.; David, W.I.F.; Johnson, S.R.; Lowton, R.L.; Sommariva, M.; Edwards, P.P. Tuning the Decomposition Temperature in Complex Hydrides: Synthesis of a Mixed Alkali Metal Borohydride. *Angew. Chem. Int. Ed.* **2008**, *47*, 2817–2819. [CrossRef]
246. Ley, M.B.; Ravnsbæk, D.B.; Filinchuk, Y.; Lee, Y.-S.; Janot, R.; Cho, Y.W.; Skibsted, J.; Jensen, T.R. $LiCe(BH_4)_3Cl$, a New Lithium-Ion Conductor and Hydrogen Storage Material with Isolated Tetranuclear Anionic Clusters. *Chem. Mater.* **2012**, *24*, 1654–1663. [CrossRef]
247. Roedern, E.; Kühnel, R.-S.; Remhof, A.; Battaglia, C. Magnesium Ethylenediamine Borohydride as Solid-State Electrolyte for Magnesium Batteries. *Sci. Rep.* **2017**, *7*, 46189. [CrossRef]
248. Amdisen, M.B.; Grinderslev, J.B.; Skov, L.N.; Jensen, T.R. Methylamine Magnesium Borohydrides as Electrolytes for All-Solid-State Magnesium Batteries. *Chem. Mater.* **2023**, *35*, 1440–1448. [CrossRef]
249. Higashi, S.; Miwa, K.; Aoki, M.; Takechi, K. A Novel Inorganic Solid State Ion Conductor for Rechargeable Mg Batteries. *Chem. Commun.* **2014**, *50*, 1320–1322. [CrossRef]
250. Le Ruyet, R.; Fleutot, B.; Berthelot, R.; Benabed, Y.; Hautier, G.; Filinchuk, Y.; Janot, R. $Mg_3(BH_4)_4(NH_2)_2$ as Inorganic Solid Electrolyte with High Mg^{2+} Ionic Conductivity. *ACS Appl. Energy Mater.* **2020**, *3*, 6093–6097. [CrossRef]
251. Yan, Y.; Dononelli, W.; Jørgensen, M.; Grinderslev, J.B.; Lee, Y.-S.; Cho, Y.W.; Černý, R.; Hammer, B.; Jensen, T.R. The Mechanism of Mg^{2+} Conduction in Ammine Magnesium Borohydride Promoted by a Neutral Molecule. *Phys. Chem. Chem. Phys.* **2020**, *22*, 9204–9209. [CrossRef]
252. Filippov, S.; Grinderslev, J.B.; Andersson, M.S.; Armstrong, J.; Karlsson, M.; Jensen, T.R.; Klarbring, J.; Simak, S.I.; Häussermann, U. Analysis of Dihydrogen Bonding in Ammonium Borohydride. *J. Phys. Chem. C* **2019**, *123*, 28631–28639. [CrossRef]
253. Jepsen, L.H.; Ban, V.; Møller, K.T.; Lee, Y.-S.; Cho, Y.W.; Besenbacher, F.; Filinchuk, Y.; Skibsted, J.; Jensen, T.R. Synthesis, Crystal Structure, Thermal Decomposition, and 11B MAS NMR Characterization of $Mg(BH_4)_2(NH_3BH_3)_2$. *J. Phys. Chem. C* **2014**, *118*, 12141–12153. [CrossRef]
254. Kisu, K.; Kim, S.; Inukai, M.; Oguchi, H.; Takagi, S.; Orimo, S. Magnesium Borohydride Ammonia Borane as a Magnesium Ionic Conductor. *ACS Appl. Energy Mater.* **2020**, *3*, 3174–3179. [CrossRef]
255. Skov, L.N.; Grinderslev, J.B.; Rosenkranz, A.; Lee, Y.; Jensen, T.R. Towards Solid-State Magnesium Batteries: Ligand-Assisted Superionic Conductivity. *Batter. Supercaps* **2022**, *5*, e202200163. [CrossRef]

256. Yan, Y.; Grinderslev, J.B.; Lee, Y.-S.; Jørgensen, M.; Cho, Y.W.; Černý, R.; Jensen, T.R. Ammonia-Assisted Fast Li-Ion Conductivity in a New Hemiammine Lithium Borohydride, $LiBH_4 \cdot 1/2NH_3$. *Chem. Commun.* **2020**, *56*, 3971–3974. [CrossRef]
257. El Kharbachi, A.; Dematteis, E.M.; Shinzato, K.; Stevenson, S.C.; Bannenberg, L.J.; Heere, M.; Zlotea, C.; Szilágyi, P.Á.; Bonnet, J.-P.; Grochala, W.; et al. Metal Hydrides and Related Materials. Energy Carriers for Novel Hydrogen and Electrochemical Storage. *J. Phys. Chem. C* **2020**, *124*, 7599–7607. [CrossRef]
258. Bannenberg, L.J.; Heere, M.; Benzidi, H.; Montero, J.; Dematteis, E.M.; Suwarno, S.; Jaroń, T.; Winny, M.; Orłowski, P.A.; Wegner, W.; et al. Metal (Boro-) Hydrides for High Energy Density Storage and Relevant Emerging Technologies. *Int. J. Hydrogen Energy* **2020**, *45*, 33687–33730. [CrossRef]
259. Hadjixenophontos, E.; Dematteis, E.M.; Berti, N.; Wołczyk, A.R.; Huen, P.; Brighi, M.; Le, T.T.; Santoru, A.; Payandeh, S.; Peru, F.; et al. Hadjixenophontos, E.; et al. A Review of the MSCA ITN ECOSTORE—Novel Complex Metal Hydrides for Efficient and Compact Storage of Renewable Energy as Hydrogen and Electricity. *Inorganics* **2020**, *8*, 17; Erratum in *Inorganics* **2020**, *8*, 63. [CrossRef]
260. Reynaud, M.; Serrano-Sevillano, J.; Casas-Cabanas, M. Imperfect Battery Materials: A Closer Look at the Role of Defects in Electrochemical Performance. *Chem. Mater.* **2023**, *35*, 3345–3363. [CrossRef]
261. Murgia, F.; Brighi, M.; Piveteau, L.; Avalos, C.E.; Gulino, V.; Nierstenhöfer, M.C.; Ngene, P.; de Jongh, P.; Černý, R. Enhanced Room-Temperature Ionic Conductivity of $NaCB_{11}H_{12}$ via High-Energy Mechanical Milling. *ACS Appl. Mater. Interfaces* **2021**, *13*, 61346–61356. [CrossRef] [PubMed]
262. Lutz, H. Ionic Motion of Tetrahedrally and Octahedrally Coordinated Lithium Ions in Ternary and Quaternary Halides. *Solid State Ion.* **1988**, *28–30*, 1282–1286. [CrossRef]
263. Zhao, F.; Alahakoon, S.H.; Adair, K.; Zhang, S.; Xia, W.; Li, W.; Yu, C.; Feng, R.; Hu, Y.; Liang, J.; et al. An Air-Stable and Li-Metal-Compatible Glass-Ceramic Electrolyte Enabling High-Performance All-Solid-State Li Metal Batteries. *Adv. Mater.* **2021**, *33*, 2006577. [CrossRef] [PubMed]
264. Sudreau, F.; Petit, D.; Boilot, J.P. Dimorphism, Phase Transitions, and Transport Properties in $LiZr_2(PO_4)_3$. *J. Solid State Chem.* **1989**, *83*, 78–90. [CrossRef]
265. Nomura, K.; Ikeda, S.; Ito, K.; Einaga, H. Framework Structure, Phase Transition and Ionic Conductivity of $MgZr_4(PO_4)_6$ and $ZnZr_4(PO_4)_6$. *J. Electroanal. Chem.* **1992**, *326*, 351–356. [CrossRef]
266. Matsuo, M.; Oguchi, H.; Sato, T.; Takamura, H.; Tsuchida, E.; Ikeshoji, T.; Orimo, S. Sodium and Magnesium Ionic Conduction in Complex Hydrides. *J. Alloys Compd.* **2013**, *580*, S98–S101. [CrossRef]
267. Zhang, H.; Liu, C.; Zheng, L.; Xu, F.; Feng, W.; Li, H.; Huang, X.; Armand, M.; Nie, J.; Zhou, Z. Lithium Bis(Fluorosulfonyl)Imide/Poly(Ethylene Oxide) Polymer Electrolyte. *Electrochim. Acta* **2014**, *133*, 529–538. [CrossRef]
268. Vasudevan, S.; Fullerton-Shirey, S.K. Effect of Nanoparticle Shape on the Electrical and Thermal Properties of Solid Polymer Electrolytes. *J. Phys. Chem. C* **2019**, *123*, 10720–10726. [CrossRef]
269. Boschin, A.; Johansson, P. Characterization of NaX (X: TFSI, FSI)—PEO Based Solid Polymer Electrolytes for Sodium Batteries. *Electrochim. Acta* **2015**, *175*, 124–133. [CrossRef]
270. Ni'mah, Y.L.; Cheng, M.-Y.; Cheng, J.H.; Rick, J.; Hwang, B.-J. Solid-State Polymer Nanocomposite Electrolyte of TiO_2/PEO/$NaClO_4$ for Sodium Ion Batteries. *J. Power Sources* **2015**, *278*, 375–381. [CrossRef]